MATCH
Communications in Mathematical and in Computer Chemistry

MATCH Commun. Math. Comput. Chem. **81** (2019) 49-90

ISSN 0340 - 6253

Type–Itemized Enumeration of [2.2]Paracyclophane Derivatives for Recasting the Concept of Stereogenic Planes by Fujita's Stereoisogram Approach

Shinsaku Fujita

Shonan Institute of Chemoinformatics and Mathematical Chemistry,

Kaneko 479-7 Ooimachi, Ashigara-Kami-Gun, Kanagawa-Ken, 258-0019 Japan

shinsaku_fujita@nifty.com

(Received July 10, 2018)

Abstract

Planar chirality of [2.2]Paracyclophane derivatives has been treated by applying Fujita's stereoisogram approach (Fujita, S. *Mathematical Stereochemistry*, De-Gruyter, 2015). By means of stereoisograms, three kinds of symmetries (chirality, *RS*-stereogenicity and sclerality) have been integrated into *RS*-stereoisomerism, which are classified into five types. Fujita's proligand method for 3D structure (Fujita, S. *Symmetry and Combinatorial Enumeration in Chemistry*, Springer-Verlag, 1991; Fujita, S. *Combinatorial Enumeration of Graphs, Three-Dimensional Structures, and Chemical Compounds*, University of Kragujevac, Faculty of Science: Kragujevac, 2013) has been extended to meet the requirement due to *RS*-stereoisomers and applied to the symmetry-itemized and type-itemized enumerations of [2.2]paracyclophane derivatives. The enumeration results are depicted by means of isomer-classification diagrams, which demonstrate isomerism of [2.2]paracyclophane derivatives.

1 Introduction

Although discontents of stereochemical terminology were pointed out by Mislow [1], several of them have not yet been avoided within the conventional approach. For example,

misleading standpoints for *R/S*-stereodescriptors of the Cahn-Ingold-Prelog (CIP) system [2, 3] have not yet been avoided, even after such decisive terms as *stereogenic* and *chirotopic* were proposed by Mislow and Siegel [4]. In fact, *IUPAC Recommendations and Preferred Names 2013*, which has recently been published as a landmark of modern stereochemistry [5], still suffers from the misleading standpoints, as discussed by the author (Fujita) in several reviews [6, 7]. In particular, chirality is presumed to be a single kind of handedness even in the IUPAC 2013 with obeying the traditional terminology.

After the proposal of stereoisogram [8, 9], the author (Fujita) has proposed a more decisive term *RS-stereogenicity* as another kind of handedness. Thereby he has proposed the stereoisogram approach for remedying discontents of stereochemical terminology [10]. In particular, he has emphasized chirality and *RS*-stereogenicity as two kinds of handedness [11]. The Aufheben of the two kinds of handedness has been summarized in a monograph [12] under the name of Fujita's stereoisogram approach.

One of the most important conclusions of Fujita's stereoisogram approach [8, 9, 12] is that stereoisograms are classified into five types (type I–type V). Thereby, a pair of stereodescriptors (*R/S*-descriptors, $R_{\mathrm{a}}/S_{\mathrm{a}}$-descriptors, and others) has been concluded to be assigned to a pair of *RS*-diastereomers, which is ascribed to *RS*-stereogenicity (the second kind of handedness) appearing in the horizontal direction of a type-I, type-III, or type-V stereoisogram. Such a pair of stereodescriptors is by no means assigned to a pair of enantiomers, which is ascribed to chirality (the first kind of handedness) appearing in the vertical direction of a type-I, type-II, or type-III stereoisogram.

The theoretical framework of Fujita's stereoisogram approach [8, 9, 12] has been found to be effective to any stereogenic units, where each stereogenic unit is replaced by a quadruplet of *RS*-stereoisomeric promolecules contained in a type-I, type-III, or type-V stereoisogram. For example, stereogenic centers of the conventional terminology are replaced by *RS*-stereogenic centers which appear in type-I, type-III, or type-V stereoisograms based on a tetrahedral skeleton [6], trigonal bipyramidal skeletons [13], an octahedral skeleton [14], and so on. In addition, stereogenic axes of the conventional terminology are replaced by *RS*-stereogenic axes which appear in type-I, type-III, or type-V stereoisograms based on an allene skeleton [15].

Fujita's stereoisogram approach has been successively applied to a cyclobutane skeleton [16], an oxirane skeleton [17], a prismane skeleton [18], a cubane skeleton [19, 20],

and so on, where type-I, type-III, or type-V stereoisograms are used to create stereodescriptors suitable for specifying the global *RS*-stereogenicity of the respective skeletons. Conventionally speaking, these skeletons are treated as the assemblies of chirality units or pseudo-asymmetric units by considering local chirality or (local) stereogenicity only. Note that the conventional CIP system does not aim at specifying global chirality nor global stereogenicity.

The remaining task is to clarify the applicability of Fujita's stereoisogram approach to stereogenic planes of the conventional terminology. Because [2.2]paracyclophane derivatives have been well-known as examples of exhibiting planar chirality or planar stereogenicity [21,22], the present paper is devoted to the application of Fujita's stereoisogram approach to a [2.2]paracyclophane skeleton. Type-I to type-V stereoisograms derived from the [2.2]paracyclophane skeleton will be enumerated combinatorially and discussed by considering chirality and *RS*-stereogenicity as two kinds of handedness.

2 Results

2.1 *RS*-Stereoisomeric Groups for Characterizing Stereoisograms

2.1.1 Reflections vs. *RS*-Permutations

The point group $\boldsymbol{D}_{2h}$ has been described in discussions on stereoisograms of ethylene derivatives [23, 24], where the four positions of an ethylene skeleton are governed by the coset representation $(\boldsymbol{C}_s''/)\boldsymbol{D}_{2h}$. Note that the subgroup $\boldsymbol{C}_s'' = \{I, \sigma_h\}$ is constructed by a reflection σ_h due to a horizontal mirror-plane.

$$\boldsymbol{D}_{2h} = \{I, C_{2(1)}, C_{2(2)}, C_{2(3)}, \sigma_h, i, \sigma_{d(1)}, \sigma_{d(2)}\}. \tag{1}$$

The same point group $\boldsymbol{D}_{2h}$ is applied to a [2.2]paracyclophane skeleton. Let us examine the eight aromatic positions, which are numbered sequentially to give a conrotatory mode along a downward view, as shown in a reference-numbered skeleton **1** (Figure 1). Then, the eight positions are governed by the coset representation $(\boldsymbol{C}_1/)\boldsymbol{D}_{2h}$.

To realize the action of the point group $\boldsymbol{D}_{2h}$, it is necessary to clarify the action of reflections contained in $\boldsymbol{D}_{2h}$. Let us examine the horizontal reflection σ_h, which is concerned with a mirror plane for reflecting the two benzene rings of the [2.2]paracyclophane skeleton **1**. Thereby, the skeleton **1** with the reference numbering is converted into a

mirror-numbered skeleton $\overline{\mathbf{1}}$. The eight positions of $\overline{\mathbf{1}}$ are attached by overlined numbers ($\overline{1}$, $\overline{2}$, etc.) in order to emphasize the action of the reflection σ_h. In addition, the permutation (product of cycles) corresponding to σ_h is also overlined to be $\overline{(1\ 5)(2\ 6)(3\ 7)(4\ 8)}$.

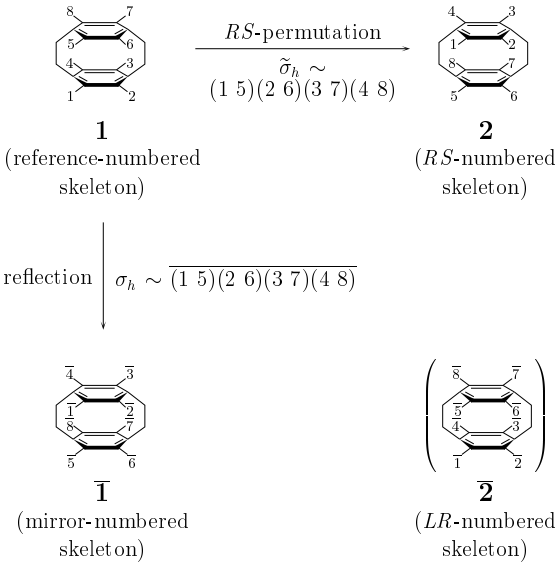

Figure 1. Action of a reflection and an RS-permutation on a reference-numbered [2.2]paracyclophane skeleton

It should be noted that Fujita's stereoisogram approach has adopted the proligand-promolecule model [25] to treat three-dimensional (3D) structures. A proligand is defined as an abstract ligand which has chirality or achirality, where its concrete 3D structure is not taken into consideration tentatively. For example, a chiral proligand p in isolation (when detached) is converted into its mirror image $\overline{\mathrm{p}}$ under the action of a reflection. An achiral proligand A in isolation remains unchanged under the action of a reflection, where A is converted into $\overline{\mathrm{A}}$ but interpreted as being $\overline{\mathrm{A}} = \mathrm{A}$. In fact, a chiral proligand p on the 1-position of **1** is converted into the enantiomeric proligand $\overline{\mathrm{p}}$ of the $\overline{1}$-position of $\overline{\mathbf{1}}$. An achiral proligand A on the 1-position of **1** is converted into $\overline{\mathrm{A}}$ of the $\overline{1}$-position of $\overline{\mathbf{1}}$, where it is regarded as being unchanged because of $\overline{\mathrm{A}} = \mathrm{A}$.

Let us next examine an RS-permutation $\widetilde{\sigma}_h$ ($\sim (1\ 5)(2\ 6)(3\ 7)(4\ 8)$), which is created by omitting an overline from the horizontal reflection σ_h. Thereby, the skeleton **1** with the reference numbering is converted into an RS-numbered skeleton **2**. The conversion from

the skeleton **1** to the *RS*-numbered skeleton **2** is regarded as a result of simultaneous rotations of the two benzene rings, although such simultaneous rotations are sterically hindered.

Under the action of the *RS*-permutation $\widetilde{\sigma}_h$, a chiral proligand p on the 1-position of **1** remain unchanged to give the proligand p of the 1-position of **2**. An achiral proligand A on the 1-position of **1** is also unchanged to give the proligand A of the 1-position of **2**.

The other reflections of $\boldsymbol{D}_{2h}$ (Eq. 1) are converted into the corresponding *RS*-permutations, where a tilde symbol is attached to show the omission of an overline. Thereby, there appears the corresponding *RS*-permutation group $\boldsymbol{D}_{2\widetilde{\sigma}}$ as follows:

$$\boldsymbol{D}_{2\widetilde{\sigma}} = \{I, C_{2(1)}, C_{2(2)}, C_{2(3)}, \widetilde{\sigma}_h, \widetilde{\imath}, \widetilde{\sigma}_{d(1)}, \widetilde{\sigma}_{d(2)}\}. \tag{2}$$

In general, the conventional methodology has used permutations (without restriction to *RS*-permutation) in place of reflections. In other words, point groups such as $\boldsymbol{D}_{2h}$ (Eq. 1) are mixed up with *RS*-permutation groups such as $\boldsymbol{D}_{2\widetilde{\sigma}}$ (Eq. 2), as pointed out in reviews [7, 11].

2.1.2 Construction of *RS*-Stereoisomeric Groups

To demonstrate how different point groups and *RS*-permutation groups are and how they interact, they are integrated into *RS*-stereoisomeric groups [8, 9, 12]. Let us examine the integration of the point group $\boldsymbol{D}_{2h}$ (Eq. 1) and *RS*-permutation group $\boldsymbol{D}_{2\widetilde{\sigma}}$ (Eq. 2). For this purpose, the reflection σ_h is applied to the *RS*-numbered skeleton **2**. Thereby, there appears another skeleton $\overline{\mathbf{2}}$, which is alternatively generated from the reference-numbered skeleton **1** by the action of $\widehat{I}$ ($\sim \overline{(1)(2)(3)(4)(5)(6)(7)(8)}$) because of $\widetilde{\sigma}_h\sigma_h = \widehat{I}$. The operation $\widehat{I}$ is called *a ligand-reflection*, so that the skeleton $\overline{\mathbf{2}}$ is called *an LR-numbered skeleton*. In a similar way to $\widetilde{\sigma}_h\sigma_h = \widehat{I}$, other ligand-reflections are generated by adding a hat symbol to the other rotations contained in $\boldsymbol{D}_2$ and by adding an overline to the corresponding products of cycles. As a result, the following ligand-reflection group $\boldsymbol{D}_{2\widehat{I}}$ is obtained:

$$\boldsymbol{D}_{2\widehat{I}} = \{I, C_{2(1)}, C_{2(2)}, C_{2(3)}, \widehat{I}, \widehat{C}_{2(1)}, \widehat{C}_{2(2)}, \widehat{C}_{2(3)}\}. \tag{3}$$

Because the point group $\boldsymbol{D}_{2h}$ (Eq. 1), the *RS*-permutation group $\boldsymbol{D}_{2\widetilde{\sigma}}$ (Eq. 2), and the ligand-reflection group $\boldsymbol{D}_{2\widehat{I}}$ (Eq. 3) have a common subgroup $\boldsymbol{D}_2$, they are integrated into the following *RS*-stereoisomeric group $\boldsymbol{D}_{2h\widetilde{\sigma}\widehat{I}}$:

$$\boldsymbol{D}_{2h\widetilde{\sigma}\widehat{I}} = \boldsymbol{D}_2 + \boldsymbol{D}_2\sigma_h + \boldsymbol{D}_2\widetilde{\sigma}_h + \boldsymbol{D}_2\widehat{I} \tag{4}$$

$$=\{I, C_{2(1)}, C_{2(2)}, C_{2(3)}, \sigma_h, i, \sigma_{d(1)}, \sigma_{d(2)},$$
$$\widetilde{\sigma}_h, \widetilde{\imath}, \widetilde{\sigma}_{d(1)}, \widetilde{\sigma}_{d(2)}, \widehat{I}, \widehat{C}_{2(1)}, \widehat{C}_{2(2)}, \widehat{C}_{2(3)}\}. \quad (5)$$

The operations of the *RS*-stereoisomeric group $\boldsymbol{D}_{2h\widetilde{\sigma}\widehat{I}}$ and the corresponding coset representation $(\boldsymbol{C}_{\widehat{I}}\backslash)\boldsymbol{D}_{2h\widetilde{\sigma}\widehat{I}}$ for the eight positions of the [2.2]paracyclophane skeleton **1** are summarized in Table 1. Note that the subgroup $\boldsymbol{C}_{\widehat{I}} = \{I, \widehat{I}\}$ is the stabilizer of each position of **1** under the action of the *RS*-stereoisomeric group $\boldsymbol{D}_{2h\widetilde{\sigma}\widehat{I}}$.

The four parts of Table 1 corresponds to the four cosets appearing in the right-hand side of Eq. 4. As a result, the left half of Table 1 indicates the eight operations of the point group $\boldsymbol{D}_{2h}$ (Eq. 1) and the corresponding coset representation $(\boldsymbol{C}_1\backslash)\boldsymbol{D}_{2h}$, where $|\boldsymbol{D}_{2h}|/|\boldsymbol{C}_1| = 8/1 = 8$. The upper half of Table 1 indicates the eight operations of the *RS*-permutation group $\boldsymbol{D}_{2\widetilde{\sigma}}$ (Eq. 2) and the corresponding coset representation $(\boldsymbol{C}_1\backslash)\boldsymbol{D}_{2\widetilde{\sigma}}$. where $|\boldsymbol{D}_{2\widetilde{\sigma}}|/|\boldsymbol{C}_1| = 8/1 = 8$. The upper-left and lower-right quadruplets of Table 1 indicate the eight operations of the ligand-reflection group $\boldsymbol{D}_{2\widehat{I}}$ (Eq. 3).

Table 1. Operations of the *RS*-stereoisomeric group $\boldsymbol{D}_{2h\widetilde{\sigma}\widehat{I}}$ and the coset representation $(\boldsymbol{C}_{\widehat{I}}\backslash)\boldsymbol{D}_{2h\widetilde{\sigma}\widehat{I}}$

operation	$(\boldsymbol{C}_{\widehat{I}}\backslash)\boldsymbol{D}_{2h\widetilde{\sigma}\widehat{I}}$	PSI	operation	$(\boldsymbol{C}_{\widehat{I}}\backslash)\boldsymbol{D}_{2h\widetilde{\sigma}\widehat{I}}$	PSI
I	(1)(2)(3)(4)(5)(6)(7)(8)	b_1^8	$\widetilde{\sigma}_h$	(1 5)(2 6)(3 7)(4 8)	b_2^4
$C_{2(3)}$	(1 3)(2 4)(5 7)(6 8)	b_2^4	$\widetilde{\imath}$	(1 7)(2 8)(3 5)(4 6)	b_2^4
$C_{2(1)}$	(1 6)(2 5)(3 8)(4 7)	b_2^4	$\widetilde{\sigma}_{d(1)}$	(1 2)(3 4)(5 6)(7 8)	b_2^4
$C_{2(2)}$	(1 8)(2 7)(3 6)(4 5)	b_2^4	$\widetilde{\sigma}_{d(2)}$	(1 4)(2 3)(5 8)(6 7)	b_2^4
σ_h	$\overline{(1\ 5)(2\ 6)(3\ 7)(4\ 8)}$	c_2^4	$\widehat{I}$	$\overline{(1)(2)(3)(4)(5)(6)(7)(8)}$	a_1^8
i	$\overline{(1\ 7)(2\ 8)(3\ 5)(4\ 6)}$	c_2^4	$\widehat{C}_{2(3)}$	$\overline{(1\ 3)(2\ 4)(5\ 7)(6\ 8)}$	c_2^4
$\sigma_{d(1)}$	$\overline{(1\ 2)(3\ 4)(5\ 6)(7\ 8)}$	c_2^4	$\widehat{C}_{2(1)}$	$\overline{(1\ 6)(2\ 5)(3\ 8)(4\ 7)}$	c_2^4
$\sigma_{d(2)}$	$\overline{(1\ 4)(2\ 3)(5\ 8)(6\ 7)}$	c_2^4	$\widehat{C}_{2(2)}$	$\overline{(1\ 8)(2\ 7)(3\ 6)(4\ 5)}$	c_2^4

2.2 Construction of Stereoisograms

2.2.1 Reference Stereoisogram for Characterizing a [2.2]-Paracyclophane Skeleton

The four skeletons shown in Figure 1 are collected and linked with equality symbols (or double-headed arrows) to give a diagram called *a reference stereoisogram*, as shown in Figure 2. For the sake of convenience, equality symbols are adopted to visualize the action

of the RS-stereoisomeric group $\boldsymbol{D}_{2h\widetilde{\sigma}\widehat{\imath}}$, where implicit hydrogen atoms are considered to occupy the eight positions. Thereby, the respective skeletons of Figure 2 behave as the representatives of the four parts of Table 1, which in turn correspond to the four cosets appearing in the right-hand side of Eq. 4.

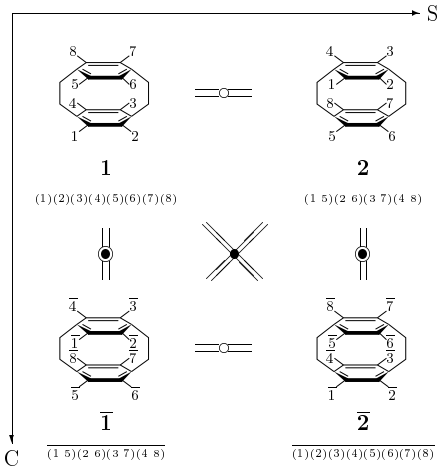

Figure 2. Reference stereoisogram for a [2.2]paracyclophane skeleton

According to Fujita's stereoisogram approach [8, 9, 12], the vertical directions of Figure 2 are described by the action of the point group $\boldsymbol{D}_{2h}$ (Eq. 1), so that they correspond to chirality/achirality from an attributive point of view or to enantiomeric/self-enantiomeric relationships from a relational point of view. Note that achirality corresponds to a self-enantiomeric relationship. The horizontal directions of Figure 2 are described by the action of the RS-permutation group $\boldsymbol{D}_{2\widetilde{\sigma}}$ (Eq. 2), so that they correspond to RS-stereogenicity/RS-astereogenicity or to RS-diastereomeric/self-RS-diastereomeric relationships. Note that RS-astereogenicity corresponds to a self-RS-diastereomeric relationship. The diagonal directions of Figure 2 are described by the action of the ligand-reflection group $\boldsymbol{D}_{2\widehat{\imath}}$ (Eq. 3), so that they correspond to sclerality/asclerality or to holantimeric/self-holantimeric relationships. Note that asclerality corresponds to a self-holantimeric relationship.

2.2.2 Type-I Stereoisograms for [2.2]-Paracyclophane Derivatives

The stereoisogram of a [2.2]paracyclophane derivative is generated by placing an appropriate set of achiral and/or chiral proligands on the eight positions of the representative skeleton **1** of the reference stereoisogram shown in Figure 2. Thereby, the four skeletons shown in Figure 2 generate four promolecules so as to give the corresponding stereoisogram, in which an equality symbol or a double-headed arrow is drawn in its vertical (attached by an encircled solid circle), horizontal (attached by an open circle), or diagonal direction (attached by a solid circle) by examining the relationships between the four promolecules.

For example, let us place one achiral proligand A at the 1-position of **1**, so as to give a promolecule **3**. Note that the remaining positions have implicit hydrogen atoms according to the composition H^7A. Thereby, there appears a type-I stereoisogram, in which equality symbols are contained in the diagonal directions, as shown in the top of Figure 3. The type-I stereoisogram is characterized to be chiral, *RS*-stereogenic, and ascleral. Note that the pairs of attributes (chirality/achirality, *RS*-stereogenicity/*RS*-astereogenicity, and sclerality/asclerality) are represented by a type index such as $[-,-,a]$, in which the symbol $-$ or a indicates the the absence or presence of the prefix a. Because of asclerality ($\mathbf{4} = \overline{\mathbf{3}}$), the *RS*-diastereomeric relationship between **3** and **4** is coincident with the enantiomeric relationship between **3** and $\overline{\mathbf{3}}$. As a result, the quadruplet of *RS*-stereoisomers of the type-I stereoisogram degenerates into a pair of enantiomers $\mathbf{3}/\overline{\mathbf{3}}$, which is coincident with a pair of *RS*-diastereomers $\mathbf{3}/\mathbf{4}$.

Group-theoretically speaking, the derivation of the type-I stereoisogram results in the restriction of the *RS*-stereoisomeric group $\boldsymbol{D}_{2h\widetilde{\sigma}\widehat{I}}$ of the skeleton **1** to the *RS*-stereoisomeric group $\boldsymbol{C}_{\widehat{I}}$ of the promolecule **3** ($\boldsymbol{C}_{\widehat{I}} = \{I, \widehat{I}\}$). Accordingly, the point group $\boldsymbol{D}_{2h}$ of the skeleton **1** is restricted to the point group $\boldsymbol{C}_1$ of the the promolecule **3** ($\leftarrow\!\odot\!\rightarrow$); the *RS*-permutation group $\boldsymbol{D}_{2\widetilde{\sigma}}$ of the skeleton **1** is restricted to the *RS*-permutation group $\boldsymbol{C}_1$ of the the promolecule **3** ($\leftarrow\!\circ\!\rightarrow$); and the ligand-reflection group $\boldsymbol{D}_{2\widehat{I}}$ is restricted to the ligand-reflection group $\boldsymbol{C}_{\widehat{I}}$ ($=\!\bullet\!=$). It should be noted that the group $\boldsymbol{C}_{\widehat{I}}$ is regarded as the ligand-reflection group of **3** under action of the ligand-reflection group $\boldsymbol{D}_{2\widehat{I}}$; and at the same time, as the *RS*-stereoisomeric group of **3** under the action of the *RS*-stereoisomeric group $\boldsymbol{D}_{2h\widetilde{\sigma}\widehat{I}}$.

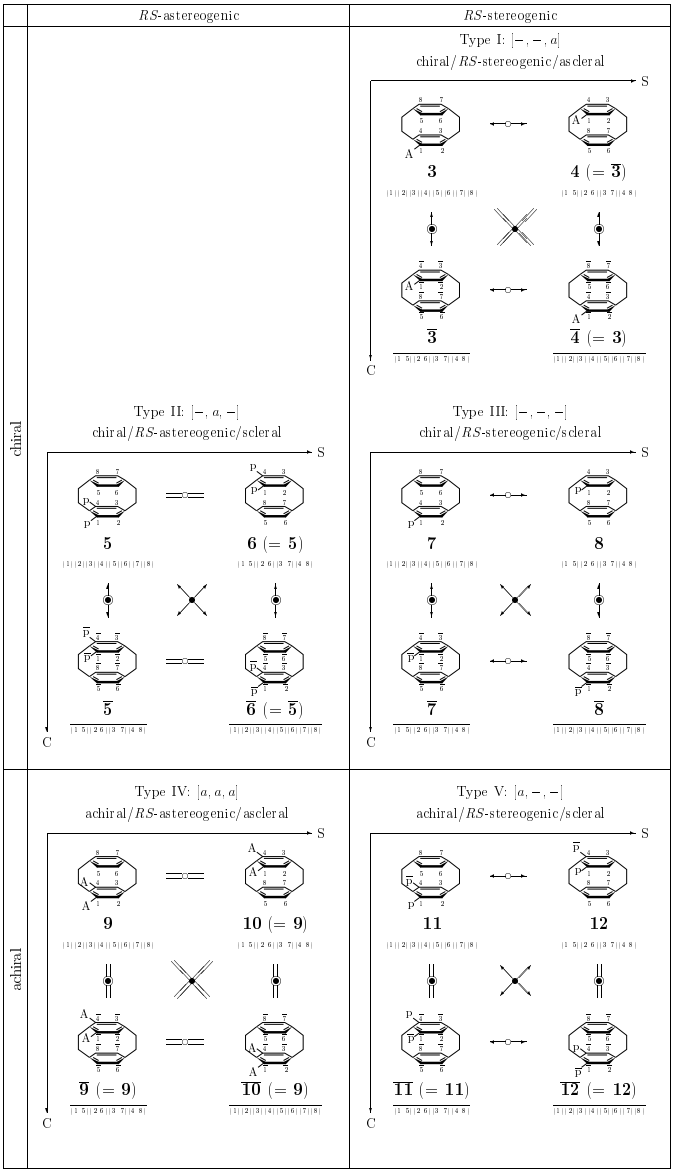

Figure 3. Sample stereoisograms of type I to type V. An uppercase letter A represents an achiral (pro)ligand in isolation. A pair of lowercase letters p/$\overline{\text{p}}$ represents a pair of enantiomeric (pro)ligands in isolation.

2.2.3 Type-II Stereoisograms for [2.2]-Paracyclophane Derivatives

Let us next place two chiral proligand p's at the 1- and 8-positions of the reference skeleton **1**, where the remaining positions have implicit hydrogen atoms according to the composition H^6p^2. Then, the reference skeleton **1** generates a promolecule **5**. Because the chiral proligand p is converted into a mirror-image proligand $\overline{p}$ by the action of a reflection or a ligand reflection, there appears a type-II stereoisogram, in which equality symbols are contained in the horizontal directions, as shown in the second row (left) of Figure 3. The type-II stereoisogram is characterized to be chiral, *RS*-astereogenic, and scleral (type index: $[-, a, -]$). Because of the *RS*-astereogenicity appearing in the horizontal direction, **5** and **6** are coincident with each other (=○=), so that they are determined to be self-*RS*-diastereomeric. In other words, the quadruplet of *RS*-stereoisomers of the type-II stereoisogram degenerates into a pair of enantiomers $\mathbf{5}/\overline{\mathbf{5}}$.

Group-theoretically speaking, the derivation of the type-II stereoisogram results in the restriction of the *RS*-stereoisomeric group $\boldsymbol{D}_{2h\widetilde{\sigma}\widehat{I}}$ of the skeleton **1** to the *RS*-stereoisomeric group $\boldsymbol{C}_{\widetilde{\sigma}}$ of the promolecule **5** ($\boldsymbol{C}_{\widetilde{\sigma}} = \{I, \widetilde{\sigma}_h\}$). Accordingly, the point group $\boldsymbol{D}_{2h}$ of the skeleton **1** is restricted to the point group $\boldsymbol{C}_1$ of the the promolecule **5** (←⊙→); the *RS*-permutation group $\boldsymbol{D}_{2\widetilde{\sigma}}$ of the skeleton **1** is restricted to the *RS*-permutation group $\boldsymbol{C}_{\widetilde{\sigma}}$ of the the promolecule **5** (=○=); and the ligand-reflection group $\boldsymbol{D}_{2\widehat{I}}$ is restricted to the ligand-reflection group $\boldsymbol{C}_1$ (←●→).

2.2.4 Type-III Stereoisograms for [2.2]-Paracyclophane Derivatives

By placing one chiral proligand p at the 1-position of the reference skeleton **1**, the reference skeleton **1** generates a promolecule **7**, which is characterized by the composition H^7p. As a result, there appears a type-III stereoisogram, in which no equality symbols are contained, as shown in the second row (right) of Figure 3. The type-III stereoisogram is characterized to be chiral, *RS*-stereogenic, and scleral (type index: $[-, -, -]$).

Group-theoretically speaking, the derivation of the type-III stereoisogram results in the restriction of the *RS*-stereoisomeric group $\boldsymbol{D}_{2h\widetilde{\sigma}\widehat{I}}$ of the skeleton **1** to the *RS*-stereoisomeric group $\boldsymbol{C}_1$ of the promolecule **7**. Accordingly, the point group $\boldsymbol{D}_{2h}$ of the skeleton **1** is restricted to the point group $\boldsymbol{C}_1$ of the the promolecule **5** (←⊙→); the *RS*-permutation group $\boldsymbol{D}_{2\widetilde{\sigma}}$ of the skeleton **1** is restricted to the *RS*-permutation group $\boldsymbol{C}_1$ of the the promolecule **5** (←○→); and the ligand-reflection group $\boldsymbol{D}_{2\widehat{I}}$ is restricted to the ligand-

reflection group $\boldsymbol{C}_1$ of the the promolecule **5** (←●→).

2.2.5 Type-IV Stereoisograms for [2.2]-Paracyclophane Derivatives

When two achiral proligands A's are placed at the 1- and 4-position of the reference skeleton **1**, the reference skeleton **1** generates a promolecule **9**, which is characterized by the composition H^6A^2. As a result, there appears a type-IV stereoisogram, in which equality symbols appear in all directions, as shown in the third row (left) of Figure 3. The type-IV stereoisogram is characterized to be achiral, *RS*-astereogenic, and ascleral (type index: $[a, a, a]$). Then, the quadruplet of *RS*-stereoisomers of the stereoisogram degenerates into a single achiral promolecule **9**.

Group-theoretically speaking, the derivation of the type-IV stereoisogram results in the restriction of the *RS*-stereoisomeric group $\boldsymbol{D}_{2h\widetilde{\sigma}\widehat{I}}$ of the skeleton **1** to the *RS*-stereoisomeric group $\boldsymbol{C}_{s\widetilde{\sigma}\widehat{I}}$ of the promolecule **9**, where we place $\boldsymbol{C}_{s\widetilde{\sigma}\widehat{I}} = \{I, \sigma_h, \widetilde{\sigma}_h, \widehat{I}\}$. Accordingly, the point group $\boldsymbol{D}_{2h}$ of the skeleton **1** is restricted to the point group $\boldsymbol{C}_s$ $(= \{I, \sigma_h\})$ of the the promolecule **9** (=⊙=); the *RS*-permutation group $\boldsymbol{D}_{2\widetilde{\sigma}}$ of the skeleton **1** is restricted to the *RS*-permutation group $\boldsymbol{C}_{\widetilde{\sigma}}$ $(= \{I, \widetilde{\sigma}_h\})$ of the the promolecule **9** (=○=); and the ligand-reflection group $\boldsymbol{D}_{2\widehat{I}}$ is restricted to the ligand-reflection group $\boldsymbol{C}_{\widehat{I}}$ $(= \{I, \widehat{I}\})$ of the the promolecule **9** (=●=).

2.2.6 Type-V Stereoisograms for [2.2]-Paracyclophane Derivatives

Let us finally place a pair of enantiomeric chiral proligands p/$\overline{\text{p}}$ at the 1- and 4-position of the reference skeleton **1**. Thereby, the reference skeleton **1** generates a promolecule **11**, which is characterized by the composition $H^6p\overline{p}$. As a result, there appears a type-V stereoisogram, which contains equality symbols along the vertical directions, as shown in the third row (right) of Figure 3. The type-V stereoisogram is characterized to be achiral, *RS*-stereogenic, and scleral (type index: $[a, -, -]$). The quadruplet of *RS*-stereoisomers of the stereoisogram degenerates into two achiral promolecules **11** and **12**.

Group-theoretically speaking, the derivation of the type-V stereoisogram results in the restriction of the *RS*-stereoisomeric group $\boldsymbol{D}_{2h\widetilde{\sigma}\widehat{I}}$ of the skeleton **1** to the *RS*-stereoisomeric group $\boldsymbol{C}''_s$ of the pair of promolecules **11**/**12**, where we place $\boldsymbol{C}''_s = \{I, \sigma_{d(2)}\}$. Accordingly, the point group $\boldsymbol{D}_{2h}$ of the skeleton **1** is restricted to the point group $\boldsymbol{C}''_s$ of the the promolecule **11** or **12** (=⊙=); the *RS*-permutation group $\boldsymbol{D}_{2\widetilde{\sigma}}$ of the skeleton **1** is restricted to the *RS*-permutation group $\boldsymbol{C}_1$ of the the promolecule **11** or **12** (←○→); and the ligand-

reflection group $\boldsymbol{D}_{2\hat{l}}$ is restricted to the ligand-reflection group $\boldsymbol{C}_1$ of the promolecule **11** or **12** (←●→).

2.3 Enumeration of [2.2]Paracyclophane Derivatives

2.3.1 Enumeration Under the Point Group $\boldsymbol{D}_{2h}$

Fujita's proligand method, which was originally developed for the purpose of gross enumerations under the action of point groups [26–29], is now applied to the enumeration of [2.2]paracyclophane derivatives. Cycle indices with chirality fittingness (CI-CFs) necessary to Fujita's proligand method are obtained by starting from products of sphericity indices (PSIs), each of which in turn is obtained by examining cycle structures of every operation, as shown in the PSI columns of Table 1. For example, the PSI of the rotation $C_{2(3)}$ (= (1 3)(2 4)(5 7)(6 8)) is calculated to be b_2^4, because a sphericity index (SI) b_2 is assigned to each hemispheric 2-cycle contained in the cycle structure 2^4. On the other hand, the PSI of the reflection σ_h (= $\overline{(1\ 5)(2\ 6)(3\ 7)(4\ 8)}$) is calculated to be c_2^4, because an SI c_2 is assigned to each enantiospheric 2-cycle contained in the cycle structure 2^4. The CI-CF for $\boldsymbol{D}_{2h}$ (CI-CF($\boldsymbol{D}_{2h}, \$_d$)) or $\boldsymbol{D}_2$ (CI-CF($\boldsymbol{D}_2, b_d$)) is calculated by summing up the PSIs of the respective operations and by dividing the resulting sum by the order ($|\boldsymbol{D}_{2h}| = 8$ or $|\boldsymbol{D}_2| = 4$) as follows:

$$\text{CI-CF}(\boldsymbol{D}_2, b_d) = \frac{1}{4}(b_1^8 + 3b_2^4) \tag{6}$$

$$\text{CI-CF}(\boldsymbol{D}_{2h}, \$_d) = \frac{1}{8}(b_1^8 + 3b_2^4 + 4c_2^4), \tag{7}$$

where the symbol $\$_d$ represents an SI, i.e., a_d for a homospheric d-cycle, c_d for an enantiospheric d-cycle, or b_d for a hemispheric d-cycle.

From Eqs. 6 and 7, CI-CF for enumerating achiral derivatives (CI-CF$^{(A)}$($\boldsymbol{D}_{2h}, \$_d$)) is derived as follows:

$$\begin{aligned}&\text{CI-CF}^{(A)}(\boldsymbol{D}_{2h}, \$_d)\\ &= 2\text{CI-CF}(\boldsymbol{D}_{2h}, \$_d) - \text{CI-CF}(\boldsymbol{D}_2, b_d) = c_2^4.\end{aligned} \tag{8}$$

On the other hand, CI-CF for enumerating enantiomeric pairs of chiral derivatives (CI-CF$^{(E)}$($\boldsymbol{D}_{2h}, \$_d$)) are derived as follows:

$$\begin{aligned}&\text{CI-CF}^{(E)}(\boldsymbol{D}_{2h}, \$_d)\\ &= \text{CI-CF}(\boldsymbol{D}_2, b_d) - \text{CI-CF}(\boldsymbol{D}_{2h}, \$_d)\end{aligned}$$

$$= \frac{1}{8}(b_1^8 + 3b_2^4 - 4c_2^4). \tag{9}$$

Suppose that the eight positions of the reference skeleton **1** are occupied by a set of eight proligands selected from the following ligand inventory:

$$\boldsymbol{L} = \{\mathrm{H}, \mathrm{A}, \mathrm{B}, \mathrm{C}, \ldots;\ \mathrm{p}/\overline{\mathrm{p}}, \mathrm{q}/\overline{\mathrm{q}}, \ldots\}, \tag{10}$$

where the uppercase letters, H, A, B, C, ..., indicate achiral proligands (H: an implicit hydrogen), while a pair of lowercase letters without and with a overline, p/$\overline{\mathrm{p}}$, q/$\overline{\mathrm{q}}$, ..., indicates a pair of enantiomeric proligands when detached. Then, the following inventory-functions are calculated:

$$a_d = \mathrm{H}^d + \mathrm{A}^d + \mathrm{B}^d + \mathrm{C}^d + \cdots \quad \text{(no lowercase terms)} \tag{11}$$

$$\begin{aligned} c_d =& \mathrm{H}^d + \mathrm{A}^d + \mathrm{B}^d + \mathrm{C}^d + \cdots \\ &+ 2\mathrm{p}^{d/2}\overline{\mathrm{p}}^{d/2} + 2\mathrm{q}^{d/2}\overline{\mathrm{q}}^{d/2} + \cdots \end{aligned} \tag{12}$$

$$\begin{aligned} b_d =& \mathrm{H}^d + \mathrm{A}^d + \mathrm{B}^d + \mathrm{C}^d + \cdots \\ &+ \mathrm{p}^d + \overline{\mathrm{p}}^d + \mathrm{q}^d + \overline{\mathrm{q}}^d + \cdots \end{aligned} \tag{13}$$

These inventory-functions are introduced into the right-hand side of each CI-CF (Eqs. 6–9). The resulting equation is expanded to give a generating function, in which the coefficient of the term $\mathrm{H}^h\mathrm{A}^a\mathrm{B}^b\mathrm{C}^c \cdots \mathrm{p}^p\overline{\mathrm{p}}^{\overline{p}}\mathrm{q}^q\overline{\mathrm{q}}^{\overline{q}} \cdots$ indicates the number of isomeric promolecules under the corresponding enumeration condition.

For the sake of simplicity, the ligand inventory $\boldsymbol{L}$ is restricted to H, A, B, and C; as well as p/$\overline{\mathrm{p}}$ and q/$\overline{\mathrm{q}}$ without losing generality. Thereby, the simplified term $\mathrm{H}^h\mathrm{A}^a\mathrm{B}^b\mathrm{C}^c\mathrm{p}^p\overline{\mathrm{p}}^{\overline{p}}\mathrm{q}^q\overline{\mathrm{q}}^{\overline{q}}$ is represented by the following partition:

$$[\theta] = [h, a, b, c; p, \overline{p}, q, \overline{q}], \tag{14}$$

where we presume the following condition:

$$h + a + b + c + p + \overline{p} + q + \overline{q} = 8. \tag{15}$$

Selected data calculated by using the CI-CFs (Eqs. 6–9) are listed in Table 2.

Table 2. Enumeration of [2.2]Paracyclophane Derivatives under Point Groups

		partition	$\boldsymbol{D}_2$	$\boldsymbol{D}_{2h}$		
				total	A	E
			(Eq. 6)	(Eq. 7)	(Eq. 8)	(Eq. 9)
$[\theta]_1$	=	[8, 0, 0, 0; 0, 0, 0, 0]	1	1	1	0
$[\theta]_2$	=	[7, 1, 0, 0; 0, 0, 0, 0]	2	1	0	1
$[\theta]_3$	=	[7, 0, 0, 0; 1, 0, 0, 0]*	2	1	0	1
$[\theta]_4$	=	[6, 2, 0, 0; 0, 0, 0, 0]	10	7	4	3
$[\theta]_5$	=	[6, 0, 0, 0; 2, 0, 0, 0]*	10	5	0	5
$[\theta]_6$	=	[6, 1, 1, 0; 0, 0, 0, 0]	14	7	0	7
$[\theta]_7$	=	[6, 1, 0, 0; 1, 0, 0, 0]*	14	7	0	7
$[\theta]_8$	=	[6, 0, 0, 0; 1, 1, 0, 0]	14	11	8	3
$[\theta]_9$	=	[6, 0, 0, 0; 1, 0, 1, 0]*	14	7	0	7
$[\theta]_{10}$	=	[5, 3, 0, 0; 0, 0, 0, 0]	14	7	0	7
$[\theta]_{11}$	=	[5, 0, 0, 0; 3, 0, 0, 0]*	14	7	0	7
$[\theta]_{12}$	=	[5, 2, 1, 0; 0, 0, 0, 0]	42	21	0	21
$[\theta]_{13}$	=	[5, 2, 0, 0; 1, 0, 0, 0]*	42	21	0	21
$[\theta]_{14}$	=	[5, 1, 0, 0; 2, 0, 0, 0]*	42	21	0	21
$[\theta]_{15}$	=	[5, 0, 0, 0; 2, 1, 0, 0]*	42	21	0	21
$[\theta]_{16}$	=	[5, 0, 0, 0; 2, 0, 1, 0]*	42	21	0	21
$[\theta]_{17}$	=	[5, 1, 1, 1; 0, 0, 0, 0]	84	42	0	42
$[\theta]_{18}$	=	[5, 1, 1, 0; 1, 0, 0, 0]*	84	42	0	42
$[\theta]_{19}$	=	[5, 1, 0, 0; 1, 1, 0, 0]	84	42	0	42
$[\theta]_{20}$	=	[5, 1, 0, 0; 1, 0, 1, 0]*	84	42	0	42
$[\theta]_{21}$	=	[5, 0, 0, 0; 1, 1, 1, 0]*	84	42	0	42
$[\theta]_{22}$	=	[4, 4, 0, 0; 0, 0, 0, 0]	22	14	6	8
$[\theta]_{23}$	=	[4, 0, 0, 0; 4, 0, 0, 0]*	22	11	0	11
$[\theta]_{24}$	=	[4, 3, 1, 0; 0, 0, 0, 0]	70	35	0	35
$[\theta]_{25}$	=	[4, 3, 0, 0; 1, 0, 0, 0]*	70	35	0	35
$[\theta]_{26}$	=	[4, 1, 0, 0; 3, 0, 0, 0]*	70	35	0	35
$[\theta]_{27}$	=	[4, 2, 2, 0; 0, 0, 0, 0]	114	63	12	51
$[\theta]_{28}$	=	[4, 2, 0, 0; 2, 0, 0, 0]*	114	57	0	57
$[\theta]_{29}$	=	[4, 0, 0, 0; 2, 2, 0, 0]	114	69	24	45
$[\theta]_{30}$	=	[4, 2, 1, 1; 0, 0, 0, 0]	210	105	0	105
$[\theta]_{31}$	=	[4, 2, 1, 0; 1, 0, 0, 0]*	210	105	0	105
$[\theta]_{32}$	=	[4, 2, 0, 0; 1, 1, 0, 0]	210	117	24	93
$[\theta]_{33}$	=	[4, 2, 0, 0; 1, 0, 1, 0]*	210	105	0	105
$[\theta]_{34}$	=	[4, 1, 1, 0; 2, 0, 0, 0]*	210	105	0	105
$[\theta]_{35}$	=	[4, 1, 0, 0; 2, 1, 0, 0]*	210	105	0	105
$[\theta]_{36}$	=	[4, 1, 0, 0; 2, 0, 1, 0]*	210	105	0	105
$[\theta]_{37}$	=	[4, 0, 0, 0; 2, 1, 1, 0]*	210	105	0	105
$[\theta]_{38}$	=	[4, 0, 0, 0; 2, 0, 1, 1]*	210	105	0	105
$[\theta]_{39}$	=	[4, 1, 1, 1; 1, 0, 0, 0]*	420	210	0	210
$[\theta]_{40}$	=	[4, 1, 1, 0; 1, 1, 0, 0]	420	210	0	210
$[\theta]_{41}$	=	[4, 1, 1, 0; 1, 0, 1, 0]*	420	210	0	210
$[\theta]_{42}$	=	[4, 1, 0, 0; 1, 1, 1, 0]*	420	210	0	210
$[\theta]_{43}$	=	[4, 0, 0, 0; 1, 1, 1, 1]	420	234	48	186

* The values should be duplicated.

The values appearing in a row having a partition with an asterisk should be duplicated. As an example, let us examine the $[\theta]_3$-row of Table 2. Because the partition $[\theta]_3$

corresponds to the term $\frac{1}{2}(\mathrm{H}^7\mathrm{p} + \mathrm{H}^7\overline{\mathrm{p}})$, the values in the $[\theta]_3$-row should be duplicated to give 4 ($= 2 \times 2$ at the $\boldsymbol{D}_2$-column), 2 ($= 1 \times 2$ at the total-column), 0 (at the A-column), and 2 ($= 1 \times 2$ at the E-column), which are consistent with the type-III stereoisogram shown in Figure 3. Thus, the value 4 indicates the presence of four derivatives, i.e., **7**, **8**, $\overline{\mathbf{7}}$, and $\overline{\mathbf{8}}$, under the point group $\boldsymbol{D}_2$; the value 2 indicates the presence of two pairs of enantiomers, i.e., $\mathbf{7}/\overline{\mathbf{7}}$ and $\mathbf{8}/\overline{\mathbf{8}}$, under the the point group $\boldsymbol{D}_{2h}$; the value 0 indicates the absence of achiral promolecules (i.e., no pairs of self-enantiomers); and the value 2 indicates the presence of two pairs of enantiomers, i.e., $\mathbf{7}/\overline{\mathbf{7}}$ and $\mathbf{8}/\overline{\mathbf{8}}$.

The values appearing in a row having a partition without an asterisk can be used as they are. For example, the values in the $[\theta]_2$-row of Table 2 are consistent with the type-I stereoisogram shown in Figure 3. Thus, the value 2 at the $\boldsymbol{D}_2$-column indicates the presence of two derivatives, i.e., **3** and $\overline{\mathbf{3}}$; the value 1 at the total-column indicates the presence of on pair of enantiomers i.e., $\mathbf{3}/\overline{\mathbf{3}}$; the value 0 at the A-column indicates the absence of achiral promolecules; and the value 1 at the E-column indicates the presence of one pair of enantiomers i.e., $\mathbf{3}/\overline{\mathbf{3}}$.

2.3.2 Enumeration Under the Subgroups of the *RS*-Stereoisomeric Group

Fujita's proligand method has been extended to cover *RS*-stereoisomeric groups [30]. In addition, combinatorial approach to group hierarchy for stereoskeletons of ligancy 4 has been investigated [31]. As a further application of Fujita's proligand method, let us examine gross enumerations of [2.2]paracyclophane derivatives under the *RS*-stereoisomeric group $\boldsymbol{D}_{2h\widetilde{\sigma}\widehat{I}}$ and under its subgroups, i.e., the *RS*-permutation group $\boldsymbol{D}_{2\widetilde{\sigma}}$ and the ligand-reflection group $\boldsymbol{D}_{2\widehat{I}}$.

In a similar way for deriving CI-CF($\boldsymbol{D}_{2h}, \$_d$) (Eq. 7), the following CI-CFs for the present targets are obtained as follows:

$$\text{CI-CF}(\boldsymbol{D}_{2\widetilde{\sigma}}, b_d) = \frac{1}{8}(b_1^8 + 7b_2^4) \tag{16}$$

$$\text{CI-CF}(\boldsymbol{D}_{2\widehat{I}}, \$_d) = \frac{1}{8}(b_1^8 + 3b_2^4 + a_1^8 + 3c_2^4) \tag{17}$$

$$\text{CI-CF}(\boldsymbol{D}_{2h\widetilde{\sigma}\widehat{I}}, \$_d) = \frac{1}{16}(b_1^8 + 7b_2^4 + a_1^8 + 7c_2^4). \tag{18}$$

The inventory-functions shown in Eqs. 11–13 are introduced into the right-hand side of each CI-CF (Eqs. 16–18). The resulting equation is expanded to give a generating function for enumerating promolecules under the respective enumeration condition. The

results are listed in Table 3, where the data of the point group $\boldsymbol{D}_{2h}$ are added at the $\boldsymbol{D}_{2h}$-column for the sake of convenience.

Table 3. Enumeration of [2.2]Paracyclophane Derivatives under the *RS*-Stereoisomeric Group and its Subgroups

partition			$\boldsymbol{D}_{2h}$ (Eq. 7)	$\boldsymbol{D}_{2\widetilde{\sigma}}$ (Eq. 16)	$\boldsymbol{D}_{2\widehat{I}}$ (Eq. 17)	$\boldsymbol{D}_{2h\widetilde{\sigma}\widehat{I}}$ (Eq. 18)
$[\theta]_1$	=	[8, 0, 0, 0; 0, 0, 0, 0]	1	1	1	1
$[\theta]_2$	=	[7, 1, 0, 0; 0, 0, 0, 0]	1	1	2	1
$[\theta]_3$	=	[7, 0, 0, 0; 1, 0, 0, 0]*	1	1	1	1/2
$[\theta]_4$	=	[6, 2, 0, 0; 0, 0, 0, 0]	7	7	10	7
$[\theta]_5$	=	[6, 0, 0, 0; 2, 0, 0, 0]*	5	7	5	7/2
$[\theta]_6$	=	[6, 1, 1, 0; 0, 0, 0, 0]	7	7	14	7
$[\theta]_7$	=	[6, 1, 0, 0; 1, 0, 0, 0]*	7	7	7	7/2
$[\theta]_8$	=	[6, 0, 0, 0; 1, 1, 0, 0]	11	7	10	7
$[\theta]_9$	=	[6, 0, 0, 0; 1, 0, 1, 0]*	7	7	7	7/2
$[\theta]_{10}$	=	[5, 3, 0, 0; 0, 0, 0, 0]	7	7	14	7
$[\theta]_{11}$	=	[5, 0, 0, 0; 3, 0, 0, 0]*	7	7	7	7/2
$[\theta]_{12}$	=	[5, 2, 1, 0; 0, 0, 0, 0]	21	21	42	21
$[\theta]_{13}$	=	[5, 2, 0, 0; 1, 0, 0, 0]*	21	21	21	21/2
$[\theta]_{14}$	=	[5, 1, 0, 0; 2, 0, 0, 0]*	21	21	21	21/2
$[\theta]_{15}$	=	[5, 0, 0, 0; 2, 1, 0, 0]*	21	21	21	21/2
$[\theta]_{16}$	=	[5, 0, 0, 0; 2, 0, 1, 0]*	21	21	21	21/2
$[\theta]_{17}$	=	[5, 1, 1, 1; 0, 0, 0, 0]	42	42	84	42
$[\theta]_{18}$	=	[5, 1, 1, 0; 1, 0, 0, 0]*	42	42	42	21
$[\theta]_{19}$	=	[5, 1, 0, 0; 1, 1, 0, 0]	42	42	42	21
$[\theta]_{20}$	=	[5, 1, 0, 0; 1, 0, 1, 0]*	42	42	42	21
$[\theta]_{21}$	=	[5, 0, 0, 0; 1, 1, 1, 0]*	42	42	42	21
$[\theta]_{22}$	=	[4, 4, 0, 0; 0, 0, 0, 0]	14	14	22	14
$[\theta]_{23}$	=	[4, 0, 0, 0; 4, 0, 0, 0]*	11	14	11	7
$[\theta]_{24}$	=	[4, 3, 1, 0; 0, 0, 0, 0]	35	35	70	35
$[\theta]_{25}$	=	[4, 3, 0, 0; 1, 0, 0, 0]*	35	35	35	35/2
$[\theta]_{26}$	=	[4, 1, 0, 0; 3, 0, 0, 0]*	35	35	35	35/2
$[\theta]_{27}$	=	[4, 2, 2, 0; 0, 0, 0, 0]	63	63	114	63
$[\theta]_{28}$	=	[4, 2, 0, 0; 2, 0, 0, 0]*	57	63	57	63/2
$[\theta]_{29}$	=	[4, 0, 0, 0; 2, 2, 0, 0]	69	63	66	42
$[\theta]_{30}$	=	[4, 2, 1, 1; 0, 0, 0, 0]	105	105	210	105
$[\theta]_{31}$	=	[4, 2, 1, 0; 1, 0, 0, 0]*	105	105	105	105/2
$[\theta]_{32}$	=	[4, 2, 0, 0; 1, 1, 0, 0]	117	105	114	63
$[\theta]_{33}$	=	[4, 2, 0, 0; 1, 0, 1, 0]*	105	105	105	105/2
$[\theta]_{34}$	=	[4, 1, 1, 0; 2, 0, 0, 0]*	105	105	105	105/2
$[\theta]_{35}$	=	[4, 1, 0, 0; 2, 1, 0, 0]*	105	105	105	105/2
$[\theta]_{36}$	=	[4, 1, 0, 0; 2, 0, 1, 0]*	105	105	105	105/2
$[\theta]_{37}$	=	[4, 0, 0, 0; 2, 1, 1, 0]*	105	105	105	105/2
$[\theta]_{38}$	=	[4, 0, 0, 0; 2, 0, 1, 1]*	105	105	105	105/2
$[\theta]_{39}$	=	[4, 1, 1, 1; 1, 0, 0, 0]*	210	210	210	105
$[\theta]_{40}$	=	[4, 1, 1, 0; 1, 1, 0, 0]	210	210	210	105
$[\theta]_{41}$	=	[4, 1, 1, 0; 1, 0, 1, 0]*	210	210	210	105
$[\theta]_{42}$	=	[4, 1, 0, 0; 1, 1, 1, 0]*	210	210	210	105
$[\theta]_{43}$	=	[4, 0, 0, 0; 1, 1, 1, 1]	234	210	228	126

* The values should be duplicated.

The values appearing in a row having a partition with an asterisk should be duplicated. For example. the $[\theta]_3$-row of Table 2 should be read as 2 ($= 1 \times 2$) at the $\boldsymbol{D}_{2h}$-column, 2 ($= 1 \times 2$) at the $\boldsymbol{D}_{2\widetilde{\sigma}}$-column, 2 ($= 1 \times 2$) at the $\boldsymbol{D}_{2\widehat{I}}$-column, and 1 ($= 1 \times \frac{1}{2}$)) at the $\boldsymbol{D}_{2h\widetilde{\sigma}\widehat{I}}$-column. These values are consistent with the type-III stereoisogram shown in Figure 3, where the term $\frac{1}{2}(\mathrm{H}^7\mathrm{p} + \mathrm{H}^7\overline{\mathrm{p}})$ is considered as a unit term for counting [2.2]paracyclophane derivatives.

Because a pair of (self-)enantiomers is counted once under a point group, the modified value 2 for $\boldsymbol{D}_{2h}$ indicates the presence of two pairs of enantiomers, i.e., $\mathbf{7}/\overline{\mathbf{7}}$ and $\mathbf{8}/\overline{\mathbf{8}}$, under the the point group $\boldsymbol{D}_{2h}$. Because a pair of (self-)RS-diastereomers is counted once under an RS-permutation group, the modified value 2 for $\boldsymbol{D}_{2\widetilde{\sigma}}$ indicates the presence of two pairs of RS-diastereomers, i.e., i.e., $\mathbf{7}/\mathbf{8}$ and $\overline{\mathbf{7}}/\overline{\mathbf{8}}$, under the RS-permutation group $\boldsymbol{D}_{2\widetilde{\sigma}}$. Because a pair of (self-)holantimers is counted once under a ligand-reflection group, the modified value 2 for $\boldsymbol{D}_{2\widehat{I}}$ indicates the presence of two pairs of holantimers i.e., $\mathbf{7}/\overline{\mathbf{8}}$ and $\mathbf{8}/\overline{\mathbf{7}}$, under the ligand-reflection group $\boldsymbol{D}_{2\widehat{I}}$. Finally, because a quadruplet of RS-stereoisomers is counted once under an RS-stereoisomeric group, the modified value 1 for $\boldsymbol{D}_{2h\widetilde{\sigma}\widehat{I}}$ indicates the presence of one quadruplet of RS-stereoisomers, i.e., $\mathbf{7}/\overline{\mathbf{7}}/\mathbf{8}/\overline{\mathbf{8}}$, under the RS-stereoisomeric group $\boldsymbol{D}_{2h\widetilde{\sigma}\widehat{I}}$.

On the other hand, the values appearing in a row having a partition without an asterisk can be used as they are. For example, the values in the $[\theta]_2$-row of Table 2 are consistent with the type-I stereoisogram shown in Figure 3. Thus, the value 1 at the $\boldsymbol{D}_{2h}$-column indicates the presence of one pair of enantiomers, i.e., $\mathbf{3}/\overline{\mathbf{3}}$, which is coincident with another pair of $\mathbf{4}/\overline{\mathbf{4}}$. The value 1 at the $\boldsymbol{D}_{2\widetilde{\sigma}}$-column indicates the presence of one pair of RS-diastereomers, i.e., $\mathbf{3}/\mathbf{4}$, which is coincident with another pair of $\overline{\mathbf{3}}/\overline{\mathbf{4}}$. The value 2 at the $\boldsymbol{D}_{2\widehat{I}}$-column indicates the presence of two pairs of self-holantimers, i.e., $\mathbf{3}/\overline{\mathbf{4}}$ and $\mathbf{4}/\overline{\mathbf{3}}$, where each pair degenerates into a single ascleral promolecule. The value 1 at the $\boldsymbol{D}_{2h\widetilde{\sigma}\widehat{I}}$-column indicates the presence of one quadruplet of RS-stereoisomers, i.e., $\mathbf{3}/\mathbf{4}/\overline{\mathbf{3}}/\overline{\mathbf{4}}$.

2.3.3 Type-Itemized Enumeration

Fujita's proligand method [26–29] has been modified to conduct the type-itemized enumeration of quadruplets of RS-stereoisomers [32, 33], which has been applied to allene derivatives and tetrahedral derivatives [32], oxirane derivatives, [33] and octahedral complexes [34]. Note that the symbols $[\theta]^*_{15}$, $[\theta]^*_{19}$, $[\theta]^*_{27}$, $[\theta]^*_{30}$, $[\theta]^*_{40}$, and $[\theta]^*_{45}$ in Table 2 of Ref. [34] should be corrected to be the symbols without an asterisk, i.e., $[\theta]_{15}$, $[\theta]_{19}$,

$[\theta]_{27}$, $[\theta]_{30}$, $[\theta]_{40}$, and $[\theta]_{45}$. Let us now apply the type-itemized enumeration method to [2.2]paracyclophane derivatives.

Table 4. Type-Itemized Enumeration of [2.2]Paracyclophane Derivatives under the *RS*-Stereoisomeric Group

partition			$\boldsymbol{D}_{2h\bar{s}\bar{t}}$ (Eq. 18)	Type I (Eq. 21)	Type II (Eq. 22)	Type III (Eq. 23)	Type IV (Eq. 24)	Type V (Eq. 25)
$[\theta]_1$	=	$[8,0,0,0;0,0,0,0]$	1	0	0	0	1	0
$[\theta]_2$	=	$[7,1,0,0;0,0,0,0]$	1	1	0	0	0	0
$[\theta]_3$	=	$[7,0,0,0;1,0,0,0]^*$	1/2	0	0	1/2	0	0
$[\theta]_4$	=	$[6,2,0,0;0,0,0,0]$	7	3	0	0	4	0
$[\theta]_5$	=	$[6,0,0,0;2,0,0,0]^*$	7/2	0	2	3/2	0	0
$[\theta]_6$	=	$[6,1,1,0;0,0,0,0]$	7	7	0	0	0	0
$[\theta]_7$	=	$[6,1,0,0;1,0,0,0]^*$	7/2	0	0	7/2	0	0
$[\theta]_8$	=	$[6,0,0,0;1,1,0,0]$	7	3	0	0	0	4
$[\theta]_9$	=	$[6,0,0,0;1,0,1,0]^*$	7/2	0	0	7/2	0	0
$[\theta]_{10}$	=	$[5,3,0,0;0,0,0,0]$	7	7	0	0	0	0
$[\theta]_{11}$	=	$[5,0,0,0;3,0,0,0]^*$	7/2	0	0	7/2	0	0
$[\theta]_{12}$	=	$[5,2,1,0;0,0,0,0]$	21	21	0	0	0	0
$[\theta]_{13}$	=	$[5,2,0,0;1,0,0,0]^*$	21/2	0	0	21/2	0	0
$[\theta]_{14}$	=	$[5,1,0,0;2,0,0,0]^*$	21/2	0	0	21/2	0	0
$[\theta]_{15}$	=	$[5,0,0,0;2,1,0,0]^*$	21/2	0	0	21/2	0	0
$[\theta]_{16}$	=	$[5,0,0,0;2,0,1,0]^*$	21/2	0	0	21/2	0	0
$[\theta]_{17}$	=	$[5,1,1,1;0,0,0,0]$	42	42	0	0	0	0
$[\theta]_{18}$	=	$[5,1,1,0;1,0,0,0]^*$	21	0	0	21	0	0
$[\theta]_{19}$	=	$[5,1,0,0;1,1,0,0]$	21	0	0	21	0	0
$[\theta]_{20}$	=	$[5,1,0,0;1,0,1,0]^*$	21	0	0	21	0	0
$[\theta]_{21}$	=	$[5,0,0,0;1,1,1,0]^*$	21	0	0	21	0	0
$[\theta]_{22}$	=	$[4,4,0,0;0,0,0,0]$	14	8	0	0	6	0
$[\theta]_{23}$	=	$[4,0,0,0;4,0,0,0]^*$	7	0	3	4	0	0
$[\theta]_{24}$	=	$[4,3,1,0;0,0,0,0]$	35	35	0	0	0	0
$[\theta]_{25}$	=	$[4,3,0,0;1,0,0,0]^*$	35/2	0	0	35/2	0	0
$[\theta]_{26}$	=	$[4,1,0,0;3,0,0,0]^*$	35/2	0	0	35/2	0	0
$[\theta]_{27}$	=	$[4,2,2,0;0,0,0,0]$	63	51	0	0	12	0
$[\theta]_{28}$	=	$[4,2,0,0;2,0,0,0]^*$	63/2	0	6	51/2	0	0
$[\theta]_{29}$	=	$[4,0,0,0;2,2,0,0]$	42	3	0	21	12	6
$[\theta]_{30}$	=	$[4,2,1,1;0,0,0,0]$	105	105	0	0	0	0
$[\theta]_{31}$	=	$[4,2,1,0;1,0,0,0]^*$	105/2	0	0	105/2	0	0
$[\theta]_{32}$	=	$[4,2,0,0;1,1,0,0]$	63	9	0	42	0	12
$[\theta]_{33}$	=	$[4,2,0,0;1,0,1,0]^*$	105/2	0	0	105/2	0	0
$[\theta]_{34}$	=	$[4,1,1,0;2,0,0,0]^*$	105/2	0	0	105/2	0	0
$[\theta]_{35}$	=	$[4,1,0,0;2,1,0,0]^*$	105/2	0	0	105/2	0	0
$[\theta]_{36}$	=	$[4,1,0,0;2,0,1,0]^*$	105/2	0	0	105/2	0	0
$[\theta]_{37}$	=	$[4,0,0,0;2,1,1,0]^*$	105/2	0	0	105/2	0	0
$[\theta]_{38}$	=	$[4,0,0,0;2,0,1,1]^*$	105/2	0	0	105/2	0	0
$[\theta]_{39}$	=	$[4,1,1,1;1,0,0,0]^*$	105	0	0	105	0	0
$[\theta]_{40}$	=	$[4,1,1,0;1,1,0,0]$	105	0	0	105	0	0
$[\theta]_{41}$	=	$[4,1,1,0;1,0,1,0]^*$	105	0	0	105	0	0
$[\theta]_{42}$	=	$[4,1,0,0;1,1,1,0]^*$	105	0	0	105	0	0
$[\theta]_{43}$	=	$[4,0,0,0;1,1,1,1]$	126	18	0	84	0	24

* The values should be duplicated.

To conduct type-itemized enumeration, the CI-CF of type V (or type IV) should be estimated. In simple cases such as an allene skeleton and a tetrahedral skeleton, the CI-CF of type V (or type IV) can be estimated manually [32, 33]. However, the present case of the [2.2]paracyclophane skeleton requires a more complicated procedure, which consists of symmetry-itemized enumeration [35, 36]. In the present article, the

procedure for estimating the CI-CF of type V (CI-CF$^{[\mathrm{V}']}(\boldsymbol{D}_{2h\widetilde{\sigma}\widehat{I}}, \$_d)$) is omitted for the sake of simplicity:

$$\begin{aligned}&\text{CI-CF}^{[\mathrm{V}']}(\boldsymbol{D}_{2h\widetilde{\sigma}\widehat{I}}, \$_d)\\ &= -\frac{1}{2}a_2^4 + \frac{1}{2}c_2^4 + \frac{3}{2}a_4^2 - \frac{3}{2}c_4^2 - \frac{3}{2}a_8 + \frac{3}{2}c_8.\end{aligned} \tag{19}$$

Thereby, the modified CI-CF of $\boldsymbol{D}_{2h}$ is obtained by starting from Eq. 7 and Eq. 19 as follows:

$$\begin{aligned}&\text{CI-CF}^{[m]}(\boldsymbol{D}_{2h}, \$_d)\\ &= \text{CI-CF}(\boldsymbol{D}_{2h}, \$_d) - \text{CI-CF}^{[\mathrm{V}']}(\boldsymbol{D}_{2h\widetilde{\sigma}\widehat{I}}, \$_d)\\ &= \frac{1}{8}b_1^8 + \frac{3}{8}b_2^4 + \frac{1}{2}a_2^4 - \frac{3}{2}a_4^2 + \frac{3}{2}c_4^2 + \frac{3}{2}a_8 - \frac{3}{2}c_8.\end{aligned} \tag{20}$$

According to Eqs. 7–11 of Ref. [33], CI-CFs for counting type-I to type-V quadruplets of RS-stereoisomers can be derived from the CI-CFs of the RS-stereoisomeric group and its subgroups. By starting from Eq. 6 and Eqs. 16–18 as well as Eq. 20 (in place of Eq. 7), CI-CFs for counting type-I to type-V quadruplets of [2.2]-paracyclophane RS-stereoisomers are calculated as follows:

$$\begin{aligned}&\text{CI-CF}^{[\mathrm{I}]}(\boldsymbol{D}_{2h\widetilde{\sigma}\widehat{I}}, \$_d)\\ &= -\text{CI-CF}^{[m]}(\boldsymbol{D}_{2h}, \$_d) + \text{CI-CF}(\boldsymbol{D}_{2\widehat{I}}, \$_d)\\ &= \frac{1}{8}a_1^8 + \frac{3}{8}c_2^4 - \frac{1}{2}a_2^4 + \frac{3}{2}a_4^2 - \frac{3}{2}c_4^2 - \frac{3}{2}a_8 + \frac{3}{2}c_8\end{aligned} \tag{21}$$

$$\begin{aligned}&\text{CI-CF}^{[\mathrm{II}]}(\boldsymbol{D}_{2h\widetilde{\sigma}\widehat{I}}, \$_d)\\ &= -\text{CI-CF}^{[m]}(\boldsymbol{D}_{2h}, \$_d) + \text{CI-CF}(\boldsymbol{D}_{2\widetilde{\sigma}}, \$_d)\\ &= \frac{1}{2}b_2^4 - \frac{1}{2}a_2^4 + \frac{3}{2}a_4^2 - \frac{3}{2}c_4^2 - \frac{3}{2}a_8 + \frac{3}{2}c_8\end{aligned} \tag{22}$$

$$\begin{aligned}&\text{CI-CF}^{[\mathrm{III}]}(\boldsymbol{D}_{2h\widetilde{\sigma}\widehat{I}}, \$_d)\\ &= \text{CI-CF}^{[m]}(\boldsymbol{D}_{2h}, \$_d) - \text{CI-CF}(\boldsymbol{D}_{2h\widetilde{\sigma}\widehat{I}}, \$_d)\\ &= \frac{1}{16}b_1^8 - \frac{1}{16}a_1^8 - \frac{1}{16}b_2^4 - \frac{7}{16}c_2^4\\ &+ \frac{1}{2}a_2^4 - \frac{3}{2}a_4^2 + \frac{3}{2}c_4^2 + \frac{3}{2}a_8 - \frac{3}{2}c_8\end{aligned} \tag{23}$$

$$\begin{aligned}&\text{CI-CF}^{[\mathrm{IV}]}(\boldsymbol{D}_{2h\widetilde{\sigma}\widehat{I}}, \$_d)\\ &= 2\text{CI-CF}^{[m]}(\boldsymbol{D}_{2h}, \$_d) - \text{CI-CF}(\boldsymbol{D}_2, b_d)\\ &= a_2^4 - 3a_4^2 + 3c_4^2 + 3a_8 - 3c_8\end{aligned} \tag{24}$$

$$\text{CI-CF}^{[\mathrm{V}]}(\boldsymbol{D}_{2h\widetilde{\sigma}\widehat{I}}, \$_d)$$

$$
\begin{aligned}
&= \text{CI-CF}(\boldsymbol{D}_2, b_d) - \text{CI-CF}^{[m]}(\boldsymbol{D}_{2h}, \$_d) - \text{CI-CF}(\boldsymbol{D}_{2\tilde{\sigma}}, \$_d) \\
&\quad - \text{CI-CF}(\boldsymbol{D}_{2\hat{I}}, \$_d) + 2\text{CI-CF}(\boldsymbol{D}_{2h\tilde{\sigma}\hat{I}}, \$_d) \\
&= \frac{1}{2}c_2^4 - \frac{1}{2}a_2^4 + \frac{3}{2}a_4^2 - \frac{3}{2}c_4^2 - \frac{3}{2}a_8 + \frac{3}{2}c_8. \qquad (25)
\end{aligned}
$$

The inventory-functions shown in Eqs. 11–13 are introduced into the right-hand side of each CI-CF (Eqs. 21–25). The resulting equation is expanded to give a generating function for enumerating type-I to type-V quadruplets of *RS*-stereoisomers. The results are listed in Table 4, where a quadruplet of *RS*-stereoisomers is counted once during the type-itemized enumeration.

The values appearing in a row having a partition with an asterisk should be duplicated. For example. the value 1/2 at the intersection of the $[\theta]_3$-row and the type-III-column in Table 4 corresponds to the term $\frac{1}{2}(\mathrm{H}^7\mathrm{p}+\mathrm{H}^7\overline{\mathrm{p}})$. This value shows the presence of one type-III quadruplet of *RS*-stereoisomers, i.e., $\mathbf{7}/\overline{\mathbf{7}}/\mathbf{8}/\overline{\mathbf{8}}$, as shown in the type-III stereoisogram of Figure 3.

On the other hand, the values appearing in a row having a partition without an asterisk can be used as they are. For example, the value 1 at the intersection of the $[\theta]_2$-row and the type-I-column in Table 4 corresponds to the term $\mathrm{H}^7\mathrm{A}$, which shows the presence of one type-I quadruplet of *RS*-stereoisomers, i.e., $\mathbf{3}/\overline{\mathbf{3}}/\mathbf{4}/\overline{\mathbf{4}}$. Note that this quadruplet under the *RS*-stereoisomeric group $\boldsymbol{D}_{2h\tilde{\sigma}\hat{I}}$ is a degenerate case derived from a pair of enantiomers $\mathbf{3}/\overline{\mathbf{3}}$, another pair of enantiomers $\mathbf{4}/\overline{\mathbf{4}}$, a pair of *RS*-diastereomers $\mathbf{3}/\mathbf{4}$, and another pair of *RS*-diastereomers $\overline{\mathbf{3}}/\overline{\mathbf{4}}$.

3 Discussions

3.1 Hierarchy for Isomerism of [2.2]Paracyclophanes

3.1.1 Isomer-Classification Diagrams and Partial Isomer-Classification Diagrams

In general, total features of isomerism have been reformed as follows:

- isomerism >
- isoskeletomerism >
- stereoisomerism >
- *RS*-stereoisomerism >

- enantiomerism (chirality), *RS*-diastereomerism (*RS*-stereogenicity), and holantimerism (sclerality),

where *isoskeletomerism* (as an intermediate concept for mediating between stereoisomerism and isomerism) [37] and *RS-stereoisomerism* (as an intermedicate concept for mediating between enantiomers and stereoisomers) [38, 39] are new matters. The total features are summarized by an isomer-classification diagram [39], which specifies a nested character of isomerism:

$$\Big(\{ \langle ([\cdots] \cdots)_{\mathrm{I-V}} \cdots \rangle \} \cdots \Big) \ . \tag{26}$$

A pair of square brackets $[\cdots]$ contains a pair of (self-)enantiomers. A pair of parentheses with the subscript I–V ($(\cdots)_{\mathrm{I-V}}$) contains a quadruplet of *RS*-stereoisomers, where the subscripts I–V are capable of specifying *RS*-diastereomerism (*RS*-stereogenicity) and holantimerism (sclerality) implicitly in addition of enantiomerism (chirality). A pair of angle brackets $\langle\cdots\rangle$ contains an equivalence class of stereoisomers, a pair of brace $\{\cdots\}$ contains an equivalence class of isoskeletomers, and each pair of large round brackets $\Big(\cdots\Big)$ contains an equivalence class of isomers.

In the present case, the results of the type-itemized enumeration are briefly represented by the following partial diagram in place of the total diagram shown above.

$$([\cdots]\cdots)_{\mathrm{I-V}} \cdots \tag{27}$$

Although *RS*-diastereomerism (*RS*-stereogenicity) and holantimerism (sclerality) are not explicitly specified in Eq. 27, the descriptions of enantiomerism (chirality) $[\cdots]$ and of type I–V are sufficient to demonstrate the total feature of a stereoisogram. For example, the degenerate feature of the quadruplet $\mathbf{3}/\overline{\mathbf{3}}/\mathbf{4}/\overline{\mathbf{4}}$ can be expressed by the partial isomer-classification diagram shown in Figure 4, where the pair of enantiomers $\mathbf{3}/\overline{\mathbf{3}}$ contained in a pair of square brackets $[\cdots]$ is selected as a representative of the quadruplet contained in a pair of parentheses with the subscript I $(\cdots)_{\mathrm{I}}$.

Such a partial isomer-classification diagram aims mainly at discussions on geometric features (chirality/achirality) of stereoisomers. On the other hand, discussions on nomenclatural features of stereoisomers (*RS*-stereogenicity/*RS*-astereogenicity) requires the implicit *RS*-diastereomerism $\mathbf{3}/\mathbf{4}$, which can be deduced in terms of the partial isomer-classification diagram (Figure 4), because the corresponding type-I stereoisogram of Figure 3 can be rationally restored.

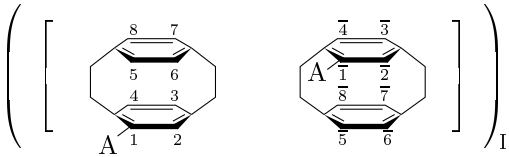

3 $\overline{\mathbf{3}}$

Figure 4. Partial isomer-classification diagram for the type-itemized enumeration of isomers having the composition H^7A, which is derived from a [2.2]paracyclophane skeleton. An uppercase letter A represents an achiral (pro)ligand in isolation.

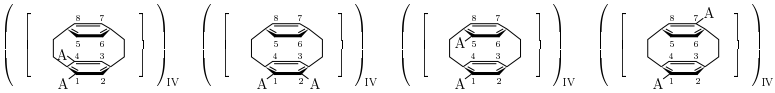

9 **13** **14** **15**

16 $\overline{\mathbf{16}}$ **17** $\overline{\mathbf{17}}$

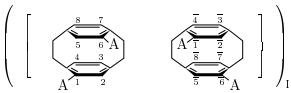

18 $\overline{\mathbf{18}}$

Figure 5. Partial isomer-classification diagram for the type-itemized enumeration of isomers having the composition H^6A^2, which are derived from a [2.2]paracyclophane skeleton. An uppercase letter A represents an achiral (pro)ligand in isolation.

3.1.2 Disubstituted [2.2]-Paracyclophanes with the Composition H^6A^2

The $[\theta]_4$-row of Table 4 indicates that the composition H^6A^2 results in the appearance of four type-IV quadruplets as well as three type-I quadruplets of *RS*-stereoisomers. Their partial isomer-classification diagram is depicted in Figure 5. Note that each of the four type-IV quadruplets degenerates to one self-enantiomeric pair (one achiral derivative, i.e., **9**, **13**, **14**, or **15**); and that each of the three type-I quadruplets degenerates to one pair of enantiomers (i.e., **16**/$\overline{\mathbf{16}}$, **17**/$\overline{\mathbf{17}}$, or **18**/$\overline{\mathbf{18}}$). It should be noted that a quadruplet of *RS*-stereoisomers is counted once in the type-itemized enumeration (Table 4). Hence, the number of pairs of parentheses with a type subscript is the number of quadruplets of the type at issue, as found in Figure 5.

Geometrically speaking, on the other hand, enumeration under point groups (Table 2) gives another viewpoint concerning [2.2]paracyclophanes. The value 10 at the intersection between the $[\theta]_4$-row and the $\boldsymbol{D}_2$-column in Table 2 indicates the number of [2.2]paracyclophanes with the composition H^6A^2 as compounds, where **9**, **13**, **14**, **15**, **17**, $\overline{\mathbf{17}}$, **16**, $\overline{\mathbf{16}}$, **18**, and $\overline{\mathbf{18}}$ are counted separately under the point group $\boldsymbol{D}_2$. The value 7 at the intersection between the $[\theta]_4$-row and the $\boldsymbol{D}_{2h}$-column (total) in Table 2 indicates the number of [2.2]paracyclophanes with the composition H^6A^2 as pairs of (self-)enantiomers (achiral derivatives and pairs of enantiomers). Because a pair of square brackets is counted once under the point group $\boldsymbol{D}_{2h}$, [**9**], [**13**], [**14**], [**15**], [**17** $\overline{\mathbf{17}}$], [**16** $\overline{\mathbf{16}}$], and [**18** $\overline{\mathbf{18}}$] are counted separately to indicate the presence of seven pairs of (self-)enantiomers. The seven pairs of (self-)enantiomers are categorized to four achiral (self-enantiomeric) [2.2]paracyclophanes ([**9**], [**13**], [**14**], and [**15**]) and three pairs of enantiomeric [2.2]paracyclophanes ([**17** $\overline{\mathbf{17}}$], [**16** $\overline{\mathbf{16}}$], and [**18** $\overline{\mathbf{18}}$]), as found at the A-column and the E-column respectively in the $[\theta]_4$-row of Table 2.

3.1.3 Disubstituted [2.2]-Paracyclophanes with the Composition H^6AB

The $[\theta]_6$-row of Table 4 shows that there appear seven type-I quadruplets having the composition H^6AB and no quadruplets of other types. Their partial isomer-classification diagram is depicted in Figure 6, where each quadruplet of *RS*-stereoisomers is counted once in the type-itemized enumeration. Hence, the number of pairs of parentheses with a type subscript I is the number of quadruplets of the type at issue, as found in Figure 6, i.e., ([**19** $\overline{\mathbf{19}}$])$_{\mathrm{I}}$, ([**20** $\overline{\mathbf{20}}$])$_{\mathrm{I}}$, ([**21** $\overline{\mathbf{21}}$])$_{\mathrm{I}}$, ([**22** $\overline{\mathbf{22}}$])$_{\mathrm{I}}$, ([**23** $\overline{\mathbf{23}}$])$_{\mathrm{I}}$, ([**24** $\overline{\mathbf{24}}$])$_{\mathrm{I}}$, and ([**25** $\overline{\mathbf{25}}$])$_{\mathrm{I}}$.

Geometrically speaking, on the other hand, enumeration under point groups (Table 2) gives another viewpoint concerning [2.2]paracyclophanes. The value 14 at the intersection between the $[\theta]_6$-row and the $\boldsymbol{D}_2$-column in Table 2 indicates the number of [2.2]paracyclophanes with the composition H^6AB as compounds, where the fourteen derivatives, **19**, $\overline{\mathbf{19}}$, **20**, $\overline{\mathbf{20}}$, **21**, $\overline{\mathbf{21}}$, **22**, $\overline{\mathbf{22}}$, **23**, $\overline{\mathbf{23}}$, **24**, $\overline{\mathbf{24}}$, **25**, and $\overline{\mathbf{25}}$, are counted separately under the point group $\boldsymbol{D}_2$. The value 7 at the intersection between the $[\theta]_6$-row and the $\boldsymbol{D}_{2h}$-column (total) in Table 2 indicates the number of [2.2]paracyclophanes with the composition H^6AB as pairs of (self-)enantiomers. The partial isomer-classification diagram (Figure 6) containing [**19** $\overline{\mathbf{19}}$], [**20** $\overline{\mathbf{20}}$], [**21** $\overline{\mathbf{21}}$], [**22** $\overline{\mathbf{22}}$], [**23** $\overline{\mathbf{23}}$], [**24** $\overline{\mathbf{24}}$], and [**25** $\overline{\mathbf{25}}$] is consistent with the enumeration result, because a pair of square brackets is counted once

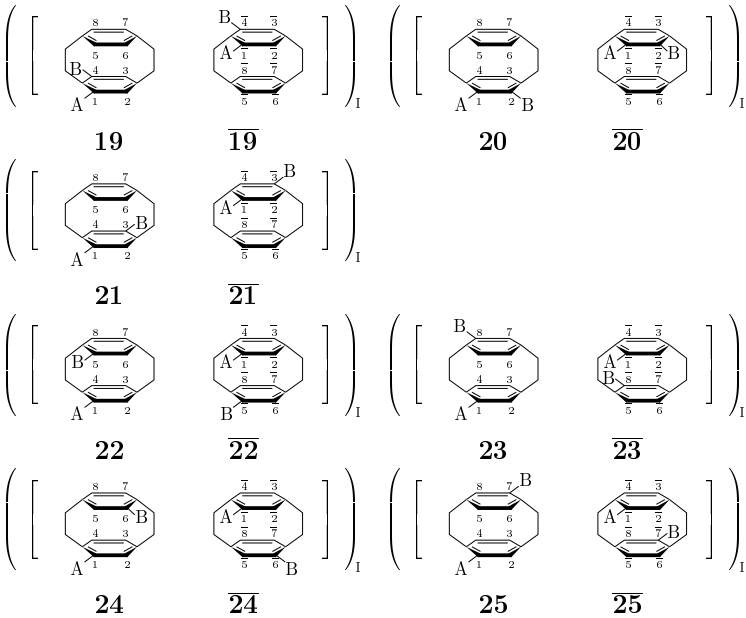

Figure 6. Partial isomer-classification diagram for the type-itemized enumeration of isomers having the composition H^6AB, which are derived from a [2.2]paracyclophane skeleton. Uppercase letters A and B represent achiral (pro)ligands in isolation.

under the point group $\boldsymbol{D}_{2h}$. All of these pairs of square brackets represent the absence of achiral derivatives and the presence of seven pairs of enantiomers in accord with the A-column (value 0) and the E-column (value 7) respectively in the $[\theta]_6$-row of Table 2.

3.1.4 Disubstituted [2.2]-Paracyclophanes with the Composition H^6Ap

The $[\theta]_7$-row of Table 4 shows the result for the composition H^6Ap, which corresponds to $\frac{1}{2}(H^6Ap + H^6A\overline{p})$. Thus, there emerge seven type-III quadruplets ($\frac{7}{2} \times 2 = 7$). Their partial isomer-classification diagram is depicted in Figure 7. Each of the seven type-III quadruplets exhibits no degeneration so as to give two pairs of enantiomers.

The isomer-classification diagram shown in Figure 7 is consistent with geometric features of the [2.2]paracyclophanes with the composition H^6Ap, which have been collected in the $[\theta]_7$-row of Table 2. The value 14 at the intersection between $[\theta]_7$-row and the $\boldsymbol{D}_2$-column shows the presence of twenty-eight [2.2]paracyclophane derivatives as compounds ($14 \times 2 = 28$ because of $\frac{1}{2}(H^6Ap + H^6A\overline{p})$). Thus, the twenty-eight derivatives,

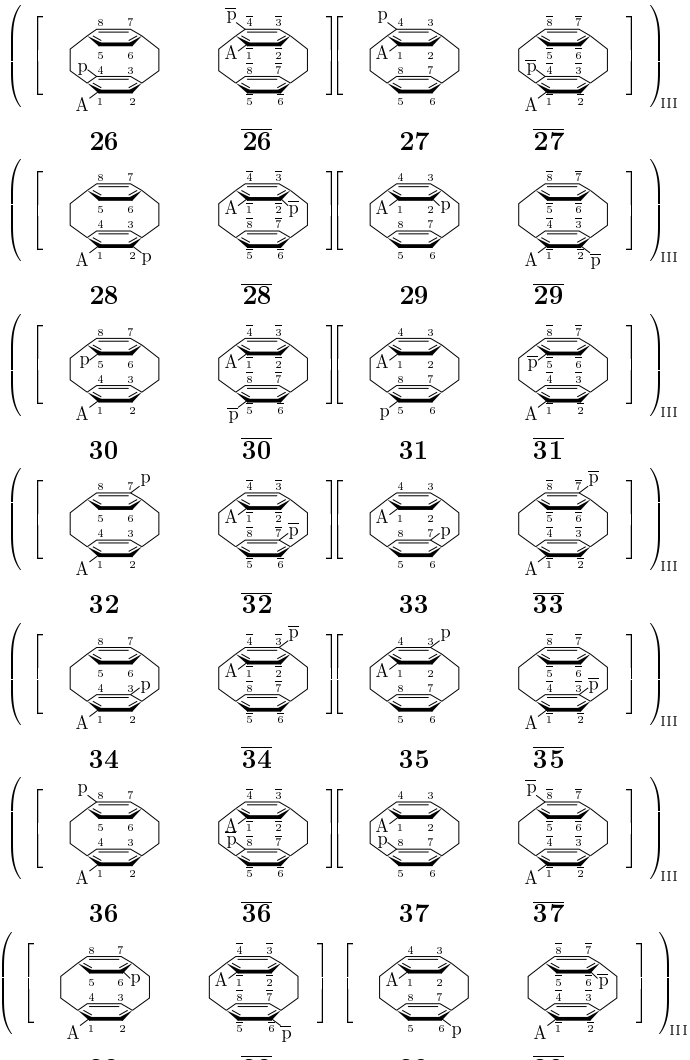

Figure 7. Partial isomer-classification diagram for the type-itemized enumeration of isomers having the composition H^6Ap, which are derived from a [2.2]paracyclophane skeleton. A pair of symbols $p/\overline{p}$ represents a pair of enantiomeric (pro)ligands in isolation.

i.e., **26**, $\overline{\mathbf{26}}$, **27**, $\overline{\mathbf{27}}$, **28**, $\overline{\mathbf{28}}$, **29**, $\overline{\mathbf{29}}$, **30**, $\overline{\mathbf{30}}$, **31**, $\overline{\mathbf{31}}$, **32**, $\overline{\mathbf{32}}$, **33**, $\overline{\mathbf{33}}$, **34**, $\overline{\mathbf{34}}$, **35**, $\overline{\mathbf{35}}$, **36**, $\overline{\mathbf{36}}$, **37**, $\overline{\mathbf{37}}$, **38**, $\overline{\mathbf{38}}$, **39**, and $\overline{\mathbf{39}}$, are counted separately under the point group $\boldsymbol{D}_2$. The value 7 at the intersection between the $[\theta]_7$-row and the $\boldsymbol{D}_{2h}$-column (total) in Table 2 shows that there appear fourteen pairs of enantiomers ($7 \times 2 = 14$ because of $\frac{1}{2}(\mathrm{H^6Ap} + \mathrm{H^6A\overline{p}})$). Because a pair of square brackets is counted once under the point group $\boldsymbol{D}_{2h}$, this value is consistent with the partial isomer-classification diagram (Figure 7). As a result, there appear fourteen pairs of enantiomeric [2.2]paracyclophanes, i.e., [**26**,$\overline{\mathbf{26}}$], [**27**, $\overline{\mathbf{27}}$], [**28**, $\overline{\mathbf{28}}$], [**29**, $\overline{\mathbf{29}}$], [**30**, $\overline{\mathbf{30}}$], [**31**, $\overline{\mathbf{31}}$], [**32**, $\overline{\mathbf{32}}$], [**33**, $\overline{\mathbf{33}}$], [**34**, $\overline{\mathbf{34}}$], [**35**, $\overline{\mathbf{35}}$], [**36**, $\overline{\mathbf{36}}$], [**37**, $\overline{\mathbf{37}}$], [**38**, $\overline{\mathbf{38}}$], and [**39**, $\overline{\mathbf{39}}$]. This result is consistent with the number 7 ($7 \times 2 = 14$) at the intersection between the $[\theta]_7$-row and the $\boldsymbol{D}_{2h}$-column (E) as well as with number 0 at the intersection between the $[\theta]_7$-row and the $\boldsymbol{D}_{2h}$-column (A) in Table 2.

3.1.5 Disubstituted [2.2]-Paracyclophanes with the Composition $\mathrm{H^6p^2}$

The $[\theta]_5$-row of Table 4 shows the result for the composition $\mathrm{H^6p^2}$, which corresponds to $\frac{1}{2}(\mathrm{H^6p^2} + \mathrm{H^6\overline{p}^2})$. Thus, there emerge four type-II quadruplets ($2 \times 2 = 4$) as well as three type-III quadruplets of *RS*-stereoisomers ($\frac{3}{2} \times 2 = 3$). Their partial isomer-classification diagram is depicted in Figure 8.

Note that each of the four type-II quadruplets degenerates to one enantiomeric pair (i.e., **5**/$\overline{\mathbf{5}}$, **40**/$\overline{\mathbf{40}}$, **41**/$\overline{\mathbf{41}}$, or **42**/$\overline{\mathbf{42}}$). On the other hand, each of the three type-III quadruplets exhibits no degeneration (i.e., **43**/$\overline{\mathbf{43}}$/**44**/$\overline{\mathbf{44}}$, **45**/$\overline{\mathbf{45}}$/**46**/$\overline{\mathbf{46}}$, or **47**/$\overline{\mathbf{47}}$/**48**/$\overline{\mathbf{48}}$), so as to give two pairs of enantiomers.

The isomer-classification diagram shown in Figure 8 is consistent with geometric features of the [2.2]paracyclophanes with the composition $\mathrm{H^6p^2}$, which have been collected in the $[\theta]_5$-row of Table 2. The value 10 at the intersection between $[\theta]_5$-row and the $\boldsymbol{D}_2$-column shows the presence of twenty [2.2]paracyclophane derivatives as compounds ($10 \times 2 = 20$ because of $\frac{1}{2}(\mathrm{H^6p^2} + \mathrm{H^6\overline{p}^2})$). Thus, the twenty derivatives, i.e., **5**, $\overline{\mathbf{5}}$, **40**, $\overline{\mathbf{40}}$, **41**, $\overline{\mathbf{41}}$, **42**, $\overline{\mathbf{42}}$, **43**, $\overline{\mathbf{43}}$, **44**, $\overline{\mathbf{44}}$, **45**, $\overline{\mathbf{45}}$, **46**, $\overline{\mathbf{46}}$, **47**, $\overline{\mathbf{47}}$, **48**, and $\overline{\mathbf{48}}$, are counted separately under the point group $\boldsymbol{D}_2$. The value 5 at the intersection between the $[\theta]_4$-row and the $\boldsymbol{D}_{2h}$-column (total) in Table 2 shows that there appear ten pairs of enantiomers ($5 \times 2 = 10$ because of $\frac{1}{2}(\mathrm{H^6p^2} + \mathrm{H^6\overline{p}^2})$). Because a pair of square brackets is counted once under the point group $\boldsymbol{D}_{2h}$, this value is consistent with the partial isomer-classification diagram (Figure 8). As a result, there appear ten pairs of enantiomeric [2.2]paracyclophanes, i.e., [**5** $\overline{\mathbf{5}}$], [**40** $\overline{\mathbf{40}}$], [**41** $\overline{\mathbf{41}}$], [**42** $\overline{\mathbf{42}}$], [**43** $\overline{\mathbf{43}}$], [**44** $\overline{\mathbf{44}}$], [**45** $\overline{\mathbf{45}}$], [**46** $\overline{\mathbf{46}}$],

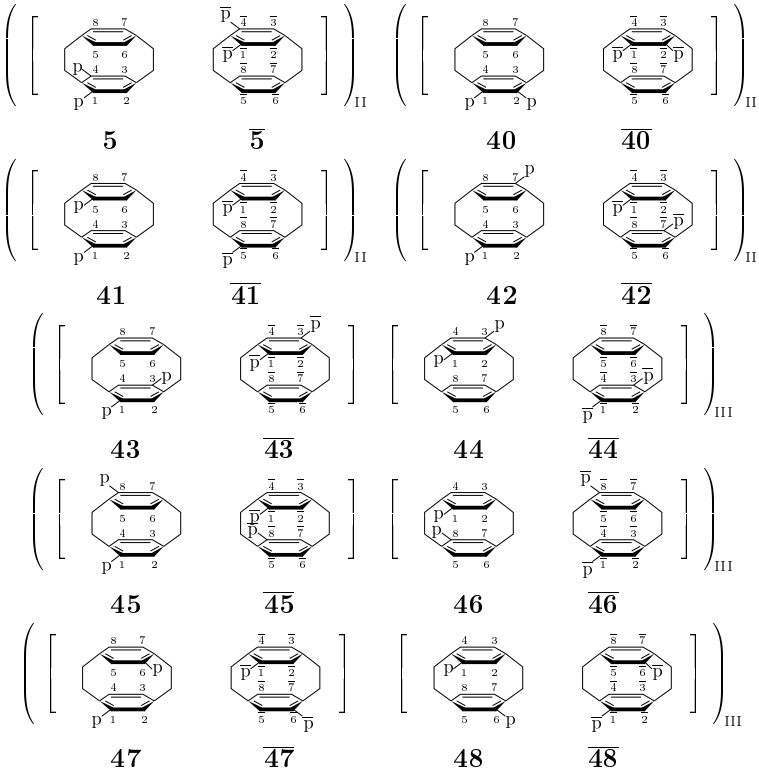

Figure 8. Partial isomer-classification diagram for the type-itemized enumeration of isomers having the composition H^6p^2, which are derived from a [2.2]paracyclophane skeleton. A pair of symbols $p/\overline{p}$ represents a pair of enantiomeric (pro)ligands in isolation.

[**47** $\overline{\mathbf{47}}$], and [**48** $\overline{\mathbf{48}}$], This result is consistent with the number 10 ($5 \times 2 = 10$) at the intersection between the $[\theta]_4$-row and the $\boldsymbol{D}_{2h}$-column (E) and with number 0 at the intersection between the $[\theta]_4$-row and the $\boldsymbol{D}_{2h}$-column (A) in Table 2.

3.1.6 Disubstituted [2.2]-Paracyclophanes with the Composition $H^6p\overline{p}$

The $[\theta]_8$-row of Table 4 shows the result for the composition $H^6p\overline{p}$. Thus, there emerge four type-V quadruplets as well as three type-I quadruplets of *RS*-stereoisomers. Their partial isomer-classification diagram is depicted in Figure 9.

Note that each of the four type-V quadruplets degenerates to a pair of *RS*-diastereomers, which are respectively achiral. For example, the stereoisogram for **11** and **12** has

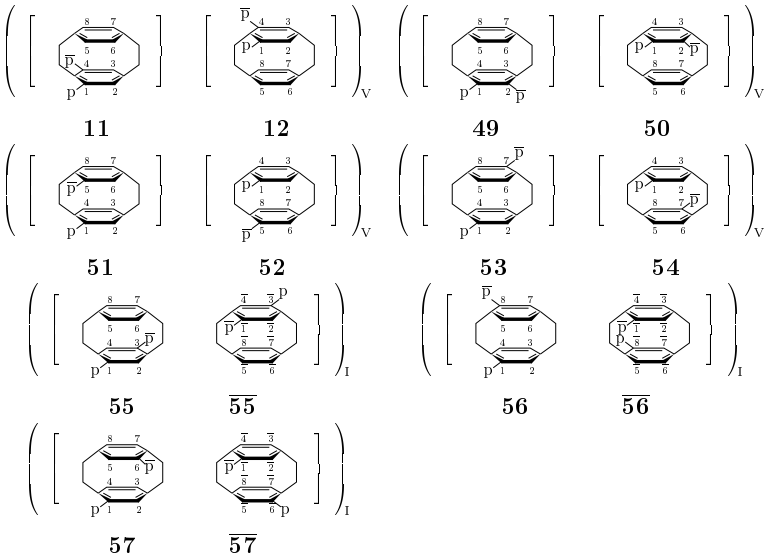

Figure 9. Partial Isomer-classification diagram for the type-itemized enumeration of isomers having the composition $H^6p\overline{p}$, which are derived from a [2.2]paracyclophane skeleton. A pair of symbols $p/\overline{p}$ represents a pair of enantiomeric (pro)ligands in isolation.

been shown in Figure 3. The achirality of **11** or **12** is expressed by a pair of square brackets with a single achiral [2.2]paracyclophane, [**11**] or [**12**], as found in the partial isomer-classification diagram (Figure 9). Then, they are surrounded by a pair of parentheses with the subscript V, i.e., ([**11**] [**12**])$_{\mathrm{V}}$, so that they are found to be *RS*-diastereomeric with each other. Similarly, such diagrams as ([**49**] [**50**])$_{\mathrm{V}}$, ([**51**] [**52**])$_{\mathrm{V}}$, and ([**53**] [**54**])$_{\mathrm{V}}$ can be interpreted by drawing the corresponding type-V stereoisograms. Each of the three type-I quadruplets degenerates to give a pair of enantiomers, as found in the corresponding diagram, ([**55** $\overline{\mathbf{55}}$])$_{\mathrm{I}}$, ([**56** $\overline{\mathbf{56}}$])$_{\mathrm{I}}$, or ([**57** $\overline{\mathbf{57}}$])$_{\mathrm{I}}$.

The $[\theta]_8$-row of Table 2 indicates the geometric features of the partial isomer-classification diagram shown in Figure 8, where enumerations under point groups are conducted. The value 14 at the intersection between $[\theta]_8$-row and the $\boldsymbol{D}_2$-column in Table 2 shows that there appear fourteen [2.2]paracyclophanes with the composition $H^6p\overline{p}$ as compounds. Thus, **11**, **12**, **49**, **50**, **51**, **52**, **53**, **54**, **55**, $\overline{\mathbf{55}}$, **56**, $\overline{\mathbf{56}}$, **57**, and $\overline{\mathbf{57}}$ are counted separately under the point group $\boldsymbol{D}_2$. The value 11 at the intersection between $[\theta]_8$-row and the $\boldsymbol{D}_{2h}$-column (total) in Table 2 shows that there appear eleven [2.2]paracyclophanes with

the composition $H^6p\overline{p}$ as pairs of (self-)enantiomers, each of which is surrounded by a pair of square brackets and counted once under the point group $\boldsymbol{D}_{2h}$. The result is consistent with the partial isomer-classification diagram (Figure 8), which contains [**11**], [**12**], [**49**], [**50**], [**51**], [**52**], [**53**], [**54**], [**55** $\overline{\mathbf{55}}$], [**56** $\overline{\mathbf{56}}$], and [**57** $\overline{\mathbf{57}}$]. These 11 pairs of (self-)enantiomers are categorized to eight pairs of self-enantiomers (eight achiral derivatives) and three pair of enantiomers. Thus, the value 8 at the intersection between $[\theta]_8$-row and the $\boldsymbol{D}_{2h}$-column (A) in Table 2 is consistent with the appearance of [**11**], [**12**], [**49**], [**50**], [**51**], [**52**], [**53**], and [**54**]; and the value 3 at the intersection between $[\theta]_8$-row and the $\boldsymbol{D}_{2h}$-column (E) in Table 2 is consistent with the appearance of [**55** $\overline{\mathbf{55}}$], [**56** $\overline{\mathbf{56}}$], and [**57** $\overline{\mathbf{57}}$].

3.2 Chirality and *RS*-Stereogenicity as Two Kinds of Handedness

3.2.1 Conventional Terminology

The terminology of the conventional stereochemistry presumes "chirality" to be a single kind of handedness:

1. The term "chirality" is defined as "The geometric property of a rigid object (or spatial arrangement of points or atoms) of being non-superposable on its mirror image; $\cdots$" [21].
2. On the other hand, the term "enantiomerism" is the relational property, because the term "enantiomerism" is defined as "The isomerism of enantiomers." [21], where the term "enantiomer" is, in turn, defined as "One of a pair of molecular entities which are mirror images of each other and non-superposable".

Thus, the term "chirality" is an attributive term which indicates the capability of generating "enantiomerism". It should be noted that the mirror image due to the conventional term "enantiomer" can be generated by both permutations (without reflections) and reflections, although such a molecular entity produced by a permutation (i.e., an *RS*-diastereomer due to Fujita's stereoisogram approach) may be coincident with the mirror image which should be generated by a reflection (i.e., an enantiomer due to Fujita's stereoisogram approach).

On the other hand, "diastereoisomerism" and "stereogenic units" are defined as follows in the conventional stereochemistry:

3. The term "diastereoisomerism" is defined as "*stereoisomerism* other than *enantiomerism*" [21], where the term "stereoisomerism" is, in turn, defined as "Isomerism due to differences in the spacial arrangement of atoms without any differences in connectivity or bond multiplicity between isomers" [21]. This means that "enantiomerism" + "diastereoisomerism" = "stereoisomerism".
4. On the other hand, the attributive terms corresponding to such relational terms as diastereoisomerism and stereoisomerism are not directly defined in the terminology of conventional stereochemistry. Instead, the term "stereogenic units" defined as "A grouping within a molecular entity that may be considered a focus of stereoisomerism. At least one of these must be present in every enantiomer (though the presence of stereogenic units does not conversely require the corresponding chemical species to be chiral). $\cdots$" [21].

Because the term "stereogenic units" means the implicit concept of "stereogenicity", the attributive term "stereogenicity" corresponds to the relational term "stereoisomerism" so long as we obey the conventional terminology. Note that the relational term "enantiomerism" corresponds to the attributive term "chirality". Hence, the attributive term ("?") corresponding to the relational term "diastereoisomerism" (= "stereoisomerism" − "enantiomerism") is not directly defined, i.e., "?" = "stereogenicity" − "chirality", in the terminology of conventional stereochemistry,

Let us examine **32** with the composition H^6Ap (Figure 7). Conventionally speaking, **32** is regarded as being stereogenic, because it is considered a focus of stereoisomerism. Note that **32** and $\overline{\mathbf{32}}$ are enantiomeric to each other. Because **32** and **33** are stereoisomeric but not enantiomeric, they are concluded to be diastereomeric to each other, if we obey the terminology of conventional stereochemistry. Similarly, **32** and $\overline{\mathbf{33}}$ are diastereomeric; **32** and **38** are diastereomeric; **32** and $\overline{\mathbf{38}}$ are diastereomeric; **32** and **39** are diastereomeric; as well as **32** and $\overline{\mathbf{39}}$ are diastereomeric. These diastereomeric relationships are not differentiated conceptually from each other. Note that the diastereomeric relationship between **32** and **33** (within pseudo-*para* derivatives) is not differentiated from the diastereomeric relationship between **32** and **38** (between a pseudo-*para* derivative and pseudo-*ortho* one).

The conventional terminology (Item 1 to 4) is based on the presumption that each molecular entity is a focus of enantiomerism, diastereoisomerism, and stereoisomerism. If

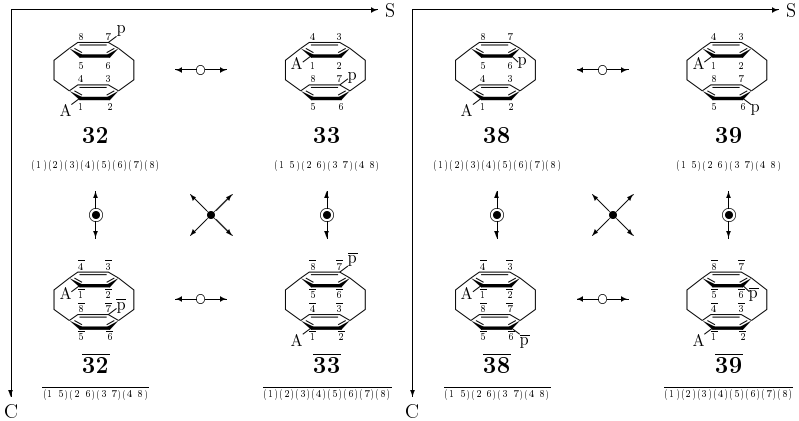

Figure 10. Type-III stereoisograms for [2.2]paracyclophane derivatives with the composition H^6Ap. These two quadruplets of *RS*-stereoisomers construct a set of stereoisomers.

each pair of enantiomers is presumed to be a focus of diastereoisomerism and stereoisomerism, a more concise scheme is obtained as follows:

$$\left\langle [\mathbf{32}\ \overline{\mathbf{32}}]\ [\mathbf{33}\ \overline{\mathbf{33}}]\ [\mathbf{38}\ \overline{\mathbf{38}}]\ [\mathbf{39}\ \overline{\mathbf{39}}] \right\rangle, \tag{28}$$

where a pair of angle brackets represents a set of stereoisomers, while a pair of square brackets represent a pair of enantiomers. As a result, we can say that two pairs of enantiomers in Eq. 28 (e.g., [**32** $\overline{\mathbf{32}}$] and [**33** $\overline{\mathbf{33}}$]) are diastereomeric to each other within the scope of the conventional terminology. Note that the diastereomeric relationship between [**32** $\overline{\mathbf{32}}$] and [**33** $\overline{\mathbf{33}}$] (within pseudo-*para* derivatives) is not differentiated from the diastereomeric relationship between [**32** $\overline{\mathbf{32}}$] and [**38** $\overline{\mathbf{38}}$] (between a pseudo-*para* derivative and pseudo-*ortho* one) even in Eq. 28.

3.2.2 Terminology Based on Fujita's stereoisogram approach

On the other hand, Fujita's stereoisogram approach [8,9,12] generates two type-III quadruplets of *RS*-stereoisomers, each of which is formulated by a stereoisogram shown in Figure 10. The type-III stereoisogram in the left of Figure 10 indicates that **32** and **33** are *RS*-diastereomeric to each other, so that **32** is *RS*-stereogenic; at the same time, **32** and $\overline{\mathbf{32}}$ are enantiomeric to each other, so that **32** is chiral. The type-III stereoisogram in the right of Figure 10 indicates that **38** and **39** are *RS*-diastereomeric to each other, so that

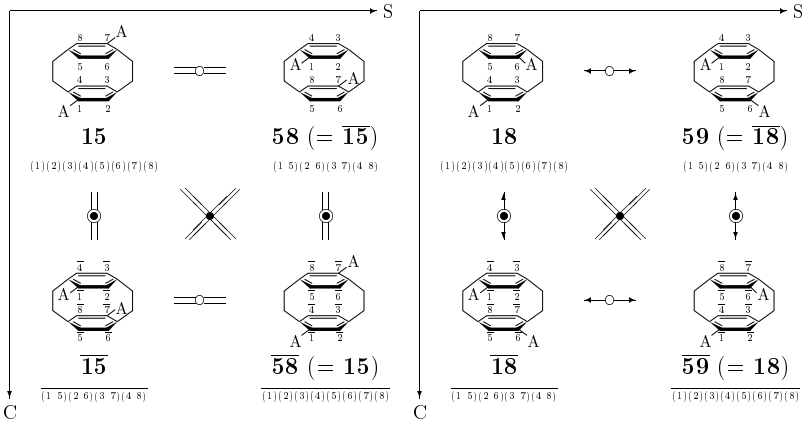

Figure 11. Type-IV and type-I stereoisograms for [2.2]paracyclophane derivatives with the composition H^6A^2. These two quadruplets of *RS*-stereoisomers construct a set of stereoisomers.

38 is *RS*-stereogenic; at the same time, **38** and $\overline{\mathbf{38}}$ are enantiomeric to each other, so that **38** is chiral. Each of the two type-III stereoisograms of Figure 10 reveals the coexistence of *RS*-stereogenicity and chirality, which are recognized to be two kinds of handedness [11].

If we adopt Fujita's stereoisogram approach in the light of Figure 10, Eq. 28 is further modified into the following scheme:

$$\left\langle \left([\mathbf{32}\ \overline{\mathbf{32}}]\ [\mathbf{33}\ \overline{\mathbf{33}}] \right)_{\mathrm{III}}\ \left([\mathbf{38}\ \overline{\mathbf{38}}]\ [\mathbf{39}\ \overline{\mathbf{39}}] \right)_{\mathrm{III}} \right\rangle . \tag{29}$$

This scheme shows a renewed viewpoint of "stereogenicity", which corresponds to a renewed diastereomeric relationship. Thus, **32** and **38** are diastereomeric to each other, where they separately belong to distinct type-III stereoisograms. Hence, **32** is stereogenic (corresponding to diastereoisomerism between the two type-III stereoisograms) in accord with Eq. 29. Note that **32** is chiral (corresponding to an enantiomeric relationship between **32** and $\overline{\mathbf{32}}$); **32** is *RS*-stereogenic (corresponding to an *RS*-diastereomeric relationship between **32** and **33**); as well as **32** is scleral (corresponding to a holantimeric relationship between **32** and $\overline{\mathbf{33}}$).

Let us next examine **15** and **18**, which have the composition H^6A^2. Fujita's stereoisogram approach [8, 9, 12] generates a type-IV quadruplet of *RS*-stereoisomers and a type-I quadruplet of *RS*-stereoisomers, as shown in the stereoisograms of Figure 11.

The type-IV stereoisogram of the left of Figure 11 reveals that **15** is achiral (a verti-

cal equality symbol corresponding to the self-enantiomeric relationship between **15** and $\overline{\mathbf{15}}$); **15** is *RS*-astereogenic (a horizontal equality symbol corresponding to the self-*RS*-diastereomeric relationship between **15** and **58**); as well as **15** is ascleral (a diagonal equality symbol corresponding to the self-holantimeric relationship between **15** and $\overline{\mathbf{58}}$). Hence the type-IV stereoisogram of the left of Figure 11 is degenerated to give a single achiral [2.2]paracyclophane derivative **15**.

The type-I stereoisogram of the right of Figure 11 reveals that **18** is chiral (corresponding to the enantiomeric relationship between **18** and $\overline{\mathbf{18}}$); **18** is *RS*-stereogenic (corresponding to the *RS*-diastereomeric relationship between **18** and **59**); as well as **18** is ascleral (a diagonal equality symbol corresponding to the self-holantimeric relationship between **18** and $\overline{\mathbf{59}}$). Hence the type-I stereoisogram of the right of Figure 11 is degenerated to give a pair of enantiomeric [2.2]paracyclophane derivatives **18** and $\overline{\mathbf{18}}$.

The behaviors described in the preceding paragraphs are summarized to give the following scheme:

$$\left\langle ([\mathbf{15}])_{\mathrm{IV}} \ \ \left([\mathbf{18}\ \overline{\mathbf{18}}]\right)_{\mathrm{I}} \right\rangle . \tag{30}$$

This scheme indicates that **15** is stereogenic and **18** is stereogenic, because **15** and **18** are diastereomeric to each other, where they belong respectively to type-IV and type-I stereoisograms.

In the light of Fujita's stereoisogram approach [8,9,12], let us compare **42** with **47** (and **48**), where they have the composition $\mathrm{H}^6\mathrm{p}^2$. As shown in the stereoisograms collected in the upper row of Figure 12, **42** generates a type-II quadruplet of *RS*-stereoisomers, while **47** and **48** generate a type-III quadruplet of *RS*-stereoisomers,

The type-II stereoisogram shown in the upper-left part of Figure 12 indicates that **42** is chiral (due to an enantiomeric relationship along the vertical direction); as well as *RS*-astereogenic (due to an *RS*-diastereomeric relationship along the horizontal direction). In contrast, the comparison between the type-II stereoisogram (for **42**) and the type-III stereoisogram (for **47**) indicates that **42** is stereogenic and **47** is stereogenic (due to a diastereomeric relationship between **42** and **47**).

Let us next compare **53** (and **54**) with **57** (and **61** (= $\overline{\mathbf{57}}$)), where they have the composition $\mathrm{H}^6\mathrm{p}\overline{\mathrm{p}}$. As shown in the stereoisograms collected in the lower row of Figure 12, **45** generates a type-V quadruplet of *RS*-stereoisomers, while **57** generates a type-I quadruplet of *RS*-stereoisomers.

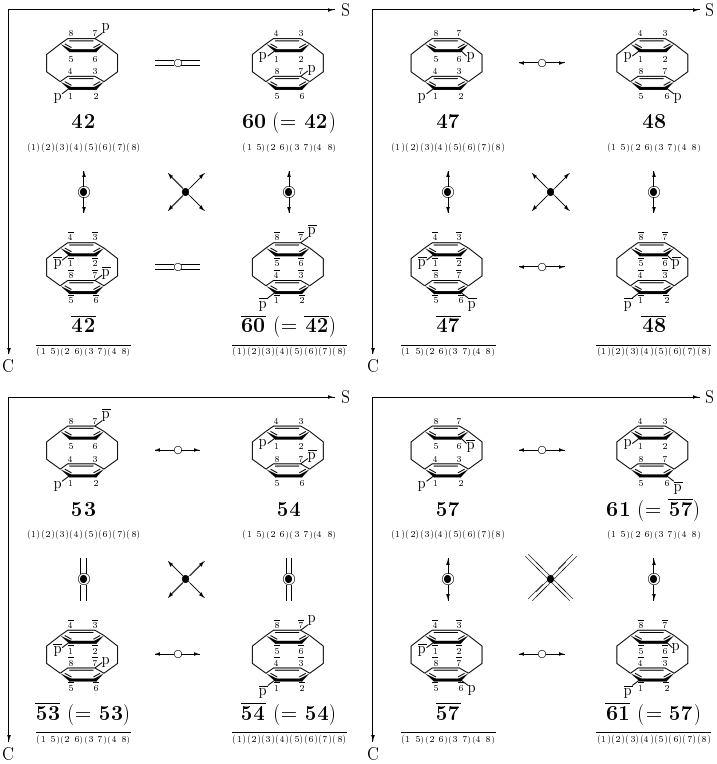

Figure 12. Type-II and type-III stereoisograms for [2.2]paracyclophane derivatives with the composition H^6p^2 (upper row) as well as Type-V and type-I stereoisograms for [2.2]paracyclophane derivatives with the composition $H^6p\overline{p}$(lower row). These four quadruplets of *RS*-stereoisomers construct a set of stereoisomers.

The type-V stereoisogram shown in the lower-left part of Figure 12 indicates that **53** is achiral (due to a self-enantiomeric relationship along the vertical direction); as well as *RS*-stereogenic (due to an *RS*-diastereomeric relationship along the horizontal direction). The type-I stereoisogram shown in the lower-right part of Figure 12 indicates that **57** is chiral (due to an enantiomeric relationship along the vertical direction); as well as *RS*-stereogenic (due to an *RS*-diastereomeric relationship along the horizontal direction). Note that the enantiomeric relationship (between **57** and $\overline{\mathbf{57}}$ (= **61**)) and the *RS*-diastereomeric relationship (between **57** and **61** (= $\overline{\mathbf{57}}$)) are coincident to each other because of the equality symbols along the diagonal direction (**61** = $\overline{\mathbf{57}}$). In contrast,

the comparison between the type-V stereoisogram (for **53**) and the type-I stereoisogram (for **57**) indicates that **53** is stereogenic and **57** is stereogenic (due to a diastereomeric relationship between **53** and **57**).

The discussions in the preceding paragraphs reveal that the four stereoisograms shown in Figure 12 satisfy the following scheme for characterizing the stereoisomerism of [2.2]paracyclophane derivatives with the compositions H^6p^2 and $H^6p\overline{p}$:

$$\langle ([\mathbf{42}\ \overline{\mathbf{42}}])_{\mathrm{II}}\ \ ([\mathbf{47}\ \overline{\mathbf{47}}]\ [\mathbf{48}\ \overline{\mathbf{48}}])_{\mathrm{III}}\ \ ([\mathbf{53}]\ [\overline{\mathbf{54}}])_{\mathrm{V}}\ \ ([\mathbf{57}\ \overline{\mathbf{57}}])_{\mathrm{I}}\rangle \tag{31}$$

Each pair of respective brackets indicates an equivalence class concerning the corresponding relationship. Any two [2.2]-derivatives can be specified by focusing the smallest equivalence class in which they are commonly contained. For example, **42** and $\overline{\mathbf{42}}$ are contained in a pair of square brackets so that they are enantiomeric to each other, where they are characterized by a type-II stereoisogram. On the other hand, **57** and $\overline{\mathbf{57}}$ are contained in a pair of square brackets so that they are enantiomeric to each other, where they are characterized by a type-I stereoisogram. Because **47** and **48** are contained commonly in a pair of round bracket with the subscript III, they are *RS*-stereoisomeric; or more specifically, they are *RS*-diastereomeric because they are interconverted by permutations (not reflections) and placed in the horizontal direction of the corresponding stereoisogram (the upper-right part of Figure 12). Because **47** and **53** are contained commonly in a pair of angle brackets, they are stereoisomeric; or more specifically, they are diastereomeric because they are interconverted by permutations (not reflections).

3.2.3 *RS*-Stereogenicity as the Second Kind of Handedness

Up to now, articles on stereochemistry have been reported on the basis of the conventional terminology, in which *chirality* is recognized to be a single kind of handedness. In contrast, Fujita's stereoisogram approach [8, 9, 12] recognizes *RS-stereogenicity* as another kind of handedness. These two kinds of handedness are integrated into *RS-stereoisomerism*, which is illustrated by a *stereoisogram* [11].

According to the conventional terminology, a pair of enantiomers [**18** $\overline{\mathbf{18}}$] (A = Br) in the left diagram of Figure 13 is characterized by a pair of R_{p} and S_{p}. Thus, R_{p}-pseudo-*ortho*-dibromo[2.2]paracyclophane is assigned to **18** and S_{p}-pseudo-*ortho*-dibromo[2.2]paracyclophane is assigned to $\overline{\mathbf{18}}$ [40]. However, Fujita's stereoisogram approach [8, 9, 12] teaches us that a pair of R_{p} and S_{p} is assigned to a pair of *RS*-diastereomers, **18** and **59**,

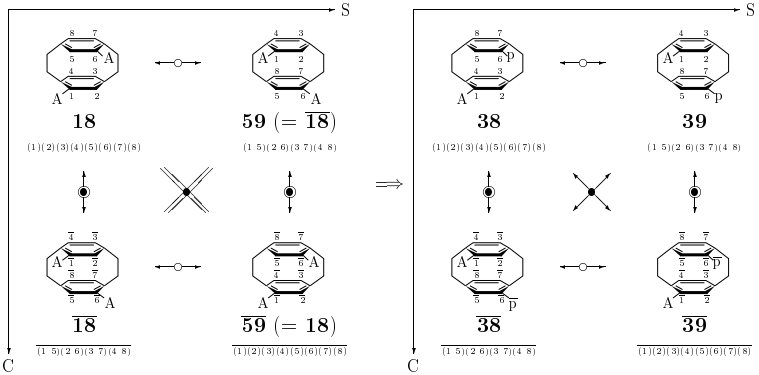

Figure 13. Conversion of type I to type III. In the light of the diagonal equality symbols in the type-I stereoisogram (left), the enantiomeric relationship (the vertical double-headed arrow) is assured to be coincident with the *RS*-diastereomeric relationship (the horizontal double-headed arrow).

which is coincident with the pair of enantiomers, **18** and $\overline{\mathbf{18}}$, because **59** is identical with $\overline{\mathbf{18}}$.

Treatment of a racemic mixture of **18** and $\overline{\mathbf{18}}$ with *n*-BuLi and (*1R,2S,5R*)-(−)-menthyl (*S*)-*p*-toluenesulfinate results in the conversion of one of the bromo groups into a sulfinyl group. Thereby, **18** (R_p) is converted into **38** (R_p, S), while $\overline{\mathbf{18}}$ (S_p) is converted into **39** (S_p, S), as shown in Figure 7 (A = Br and p = –SO–*p*-Tol-(*S*) [40]. Thus, a pair of *RS*-descriptors $R_\mathrm{p}/S_\mathrm{p}$ is assigned to a pair of enantiomers, **18**/$\overline{\mathbf{18}}$, while a pair of *RS*-descriptors $R_\mathrm{p}, S/S_\mathrm{p}, S$ is assigned to a pair of "diastereomers" (*RS*-diastereomers) **38**/**39**, if we obey the conventional terminology. In contrast, Fujita's stereoisogram approach emphasizes *RS*-stereogenicity as the second kind of handedness. Thus, a pair of *RS*-descriptors $R_\mathrm{p}/S_\mathrm{p}$ is assigned to a pair of *RS*-diastereomers **18**/**59**(= $\overline{\mathbf{18}}$); and at the same time, a pair of *RS*-descriptors $R_\mathrm{p}, S/S_\mathrm{p}, S$ is assigned to a pair of *RS*-diastereomers **38**/**39**, if we obey Fujita's stereoisogram approach. By referring to the type-I stereoisogram shown in the left of Figure 13, the enantiomeric relationship between **18** and $\overline{\mathbf{18}}$ is assured to be coincident with the *RS*-diastereomeric relationship between **18** and **59**.

As a result, the conversion shown in Figure 13 is characterized by *RS*-stereogenicity as the second kind of handedness. Thus, the pair of *RS*-diastereomers **18**/**59**(= $\overline{\mathbf{18}}$) is converted into a pair of *RS*-diastereomers **38**/**39**, if we obey Fujita's stereoisogram approach.

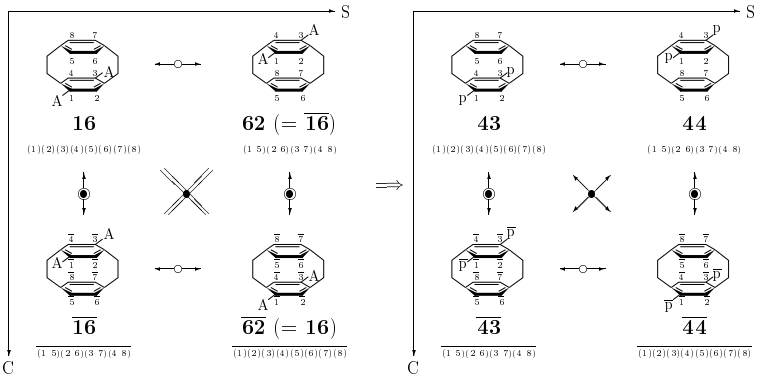

Figure 14. Conversion of type I to type III. The diagonal equality symbols in the type-I stereoisogram (left) shows that the enantiomeric relationship (the vertical double-headed arrow) is coincident with the *RS*-diastereomeric relationship (the horizontal double-headed arrow).

Figure 14 shows another example for illustrating the conversion of type-I to type-III stereoisograms. The enantiomeric pair of [2.2]paracyclophane-4,7-dicarboxylic acids [**16** $\overline{\mathbf{16}}$] (in which A = COOH) was reported to react with *S*-phenylethylamine, so that an *RS*-diastereomeric pair of **43**/**44** (in which p = CONH-CH(CH_3)Ph having an *S*-phenylethylamine moiety) is generated [41]. As a result, the diastereomeric excess of the diastereomeric pair of **43**/**44** was determined to estimate the enantiomeric excess (ee) value of the pair [**16** $\overline{\mathbf{16}}$] (A = COOH).

According to the conventional stereochemistry, the enantiomeric pair of [**16** $\overline{\mathbf{16}}$] (in which A = COOH) is concerned to chirality (due to geometric aspect), while the diastereomeric pair of **43**/**44** is concerned with stereogenicity (due to stereoisomeric aspect).

If we obey Fujita's stereoisogram approach, a pair of *RS*-descriptors $R_{\mathrm{p}}/S_{\mathrm{p}}$ is assigned to a pair of *RS*-diastereomers **16**/**62**(= $\overline{\mathbf{16}}$); and at the same time, a pair of *RS*-descriptors $R_{\mathrm{p}}, S/S_{\mathrm{p}}, S$ is assigned to a pair of *RS*-diastereomers **43**/**44**. Note that the enantiomeric relationship between **16** and $\overline{\mathbf{16}}$ is coincident with the *RS*-diastereomeric relationship between **16** and **62** by referring to the type-I stereoisogram shown in the left of Figure 14. As a result, the assignment of *RS*-descriptors $R_{\mathrm{p}}/S_{\mathrm{p}}$ is concluded to be based on *RS*-stereogenicity (the second kind of handedness), not on chirality (the first kind of handedness).

4 Conclusion

[2.2]Paracyclophane derivatives have been combinatorially enumerated by means of Fujita's proligand method [26–29], which is capable of enumerating 3D structures as well as graphs. Planar chirality of [2.2]Paracyclophane derivatives has been treated by applying Fujita's stereoisogram approach, [8, 9, 12] where two kinds of handedness (chirality due to a point group $\boldsymbol{D}_{2h}$ and *RS*-stereogenicity due to an *RS*-permutation group $\boldsymbol{D}_{2\widetilde{\sigma}}$) are taken into consideration. By means of stereoisograms which generate another symmetry (sclerality due to a ligand-reflection group $\boldsymbol{D}_{2\widehat{I}}$), these symmetries (chirality, *RS*-stereogenicity, and sclerality) are integrated into *RS*-stereoisomerism, which corresponds to an *RS*-stereoisomeric group $\boldsymbol{D}_{2h\widetilde{\sigma}\widehat{I}}$. [2.2]Paracyclophane derivatives have been enumerated under point groups ($\subset \boldsymbol{D}_{2h}$), and under *RS*-stereoisomeric groups ($\subset \boldsymbol{D}_{2h\widetilde{\sigma}\widehat{I}}$). [2.2]Paracyclophane derivatives have been classified into five types by drawing type-I to type-V stereoisograms. They have been enumerated in a type-itemized fashion. The enumeration results are depicted by means of isomer-classification diagrams [39], which demonstrate isomerism of [2.2]paracyclophane derivatives.

References

[1] K. Mislow, Stereochemical terminology and its discontents, *Chirality* **14** (2002) 126–134.

[2] R. S. Cahn, C. K. Ingold, V. Prelog, Specification of molecular chirality, *Angew. Chem. Int. Ed. Eng.* **5** (1966) 385–415.

[3] V. Prelog, G. Helmchen, Basic principles of the CIP-system and proposal for a revision, *Angew. Chem. Int. Ed. Eng.* **21** (1982) 567–583.

[4] K. Mislow, J. Siegel, Stereoisomerism and local chirality, *J. Am. Chem. Soc.* **106** (1984) 3319–3328.

[5] H. A. Favre, W. H. Powell, *Nomenclature of Organic Chemistry: IUPAC Recommendations and Preferred Names 2013*, Royal Soc. Chem., Cambridge, 2013.

[6] S. Fujita, Stereoisograms for reorganizing the theoretical foundations of stereochemistry and stereoisomerism: II. Rational avoidance of misleading standpoints for *R/S*-

stereodescriptors of the Cahn–Ingold–Prelog system, *Tetrahedron: Asymmetry* **25** (2014) 1169–1189.

[7] S. Fujita, Conceptual defects of modern stereochemistry. Comprehensive remedy by stereoisograms based on rs-stereoisomerism for mediating between enantiomerism and stereoisomerism, *Tetrahedron: Asymmetry* **28** (2017) 1–33.

[8] S. Fujita, Stereogenicity revisited. Proposal of holantimers for comprehending the relationship between stereogenicity and chirality, *J. Org. Chem.* **69** (2004) 3158–3165.

[9] S. Fujita, Pseudoasymmetry, stereogenicity, and the *RS*-nomenclature comprehended by the concepts of holantimers and stereoisograms, *Tetrahedron* **60** (2004) 11629–11638.

[10] S. Fujita, The stereoisogram approach for remedying discontents of stereochemical terminology, *Tetrahedron: Asymmetry* **25** (2014) 1612–1623.

[11] S. Fujita, Chirality and *RS*-stereogenicity as two kinds of handedness. Their aufheben by Fujitafs stereoisogram approach for giving new insights into classification of isomers, *Bull. Chem. Soc. Jpn.* **89** (2016) 987–1017.

[12] S. Fujita, *Mathematical Stereochemistry*, De Gruyter, Berlin, 2015.

[13] S. Fujita, Stereoisograms of trigonal bipyramidal compounds: II. *RS*-stereogenicity/*RS*-stereoisomerism versus stereogenicity/stereoisomerism, leading to a revised interpretation of Berry's pseudorotation, *J. Math. Chem.* **50** (2012) 1815–1860.

[14] S. Fujita, Stereoisograms of octahedral complexes. II. *RS*-Stereogenicity vs. stereogenicity as well as *RS*-stereoisomerism vs. stereoisomerism, *MATCH Commun. Math. Comput. Chem.* **71** (2014) 537–574.

[15] S. Fujita, Symmetry-itemized enumeration of *RS*-stereoisomers of allenes. II. The partial–cycle–index method of the USCI approach combined with the stereoisogram approach, *J. Math. Chem.* **52** (2014) 1751–1793.

[16] S. Fujita, Correlation diagrams of stereoisograms for characterizing stereoisomers of cyclobutane derivatives, *J. Math. Chem.* **47** (2010) 145–166.

[17] S. Fujita, Stereoisograms for three-membered heterocycles: II. Chirality,*RS*-stereogenicity, and *ortho*-stereogenicity on the basis of the proligand-promolecule model, *J. Math. Chem.* **53** (2015) 305–352.

[18] S. Fujita, Importance of the proligand–promolecule model in stereochemistry. II. the stereoisogram approach to stereoisomeric features of prismane derivatives, *J. Math. Chem.* **50** (2012) 2168–2201.

[19] S. Fujita, Stereoisograms of cubane derivatives, *Bull. Chem. Soc. Jpn.* **88** (2015) 1653–1679.

[20] S. Fujita, Systematic enumeration and symmetries of cubane derivatives, *Chem. Rec.* **16** (2016) 1116–1163.

[21] IUPAC Organic Chemistry Division, Basic terminology of stereochemistry (IUPAC recommendations 1996), *Pure Appl. Chem.* **68** (1996) 2193–2222.

[22] B. Testa, Organic stereochemistry. Part 3. Other stereogenic elements: Axes of chirality, planes of chirality, helicity, and (*E,Z*)-diastereoisomerism, *Helv. Chim. Acta* **96** (2013) 351–374.

[23] S. Fujita, Stereogenicity/astereogenicity as global/local permutation–group symmetry and relevant concepts for restructuring stereochemistry, *J. Math. Chem.* **33** (2003) 113–143.

[24] S. Fujita, Group-theoretical discussion on the *E/Z*-nomenclature for ethylene derivatives. Discrimination between *RS*-stereoisomeric groups and stereoisomeric groups, *J. Chem. Inf. Comput. Sci.* **44** (2004) 1719–1726.

[25] S. Fujita, Promolecules for characterizing stereochemical relationships in non-rigid molecules, *Tetrahedron* **47** (1991) 31–46.

[26] S. Fujita, Graphs to chemical structures 1. Sphericity indices of cycles for stereochemical extension of Pólya's theorem, *Theor. Chem. Acc.* **113** (2005) 73–79.

[27] S. Fujita, Graphs to chemical structures 2. Extended sphericity indices of cycles for stereochemical extension of Pólya's coronas, *Theor. Chem. Acc.* **113** (2005) 80–86.

[28] S. Fujita, Graphs to chemical structures 3. General theorems with the use of different sets of sphericity indices for combinatorial enumeration of nonrigid stereoisomers, *Theor. Chem. Acc.* **115** (2006) 37–53.

[29] S. Fujita, *Combinatorial Enumeration of Graphs, Three–Dimensional Structures, and Chemical Compounds*, Univ. Kragujevac, Kragujevac, 2013.

[30] S. Fujita, Computer-oriented representations of *RS*-stereoisomeric groups and cycle indices with chirality fittingness (CI-CFs) calculated by the gap system. enumeration of *RS*-stereoisomers by Fujita's proligand method, *MATCH Commun. Math. Comput. Chem.* **77** (2017) 443–478.

[31] S. Fujita, Combinatorial approach to group hierarchy for stereoskeletons of ligancy 4, *J. Math. Chem.* **53** (2015) 1010–1053.

[32] S. Fujita, Type-itemized enumeration of quadruplets of rs-stereoisomers. I. Cycle indices with chirality fittingness modulated by type-IV quadruplets, *J. Math. Chem.* **54** (2016) 286–309.

[33] S. Fujita, Type-itemized enumeration of quadruplets of *RS*-stereoisomers: II. Cycle indices with chirality fittingness modulated by type-V quadruplets, *J. Math. Chem.* **54** (2016) 310–330.

[34] S. Fujita, Type-itemized enumeration of *RS*-stereoisomers of octahedral complexes, *Iran. J. Math. Chem.* **7** (2016) 113–153; The symbols $[\theta]^*_{15}$, $[\theta]^*_{19}$, $[\theta]^*_{27}$, $[\theta]^*_{30}$, $[\theta]^*_{40}$, and $[\theta]^*_{45}$ in Table 2 should be corrected to be $[\theta]_{15}$, $[\theta]_{19}$, $[\theta]_{27}$, $[\theta]_{30}$, $[\theta]_{40}$, and $[\theta]_{45}$.

[35] S. Fujita, Symmetry–itemized enumeration of *RS*-stereoisomers of allenes. I. The fixed-point matrix method of the USCI approach combined with the stereoisogram approach, *J. Math. Chem.* **52** (2014) 1717–1750.

[36] S. Fujita, Stereoisograms for three-membered heterocycles: I. Symmetry–itemized enumeration of oxiranes under an *RS*-stereoisomeric group, *J. Math. Chem.* **53** (2015) 260–304.

[37] S. Fujita, Isoskeletomerism as an intermediate concept for mediating between stereoisomerism and isomerism. A remedy for conceptual defects of organic chemistry, *Tetrahedron: Asymmetry* **28** (2017) 900–920.

[38] S. Fujita, Misleading classification of isomers and stereoisomers in organic chemistry, *Bull. Chem. Soc. Jpn.* **87** (2014) 1367–1378.

[39] S. Fujita, Classification of stereoisomers. Flowcharts without and with the intermediate concept of *RS*-stereoisomers for mediating between enantiomers and stereoisomers, *Tetrahedron: Asymmetry* **27** (2016) 43–62.

[40] Y. Morisaki, R. Hifumi, L. Lin, K. Inoshita, Y. Chujo, Practical optical resolution of planar chiral pseudo-*ortho*-disubstituted [2.2]paracyclophane, *Chem. Lett.* **41** (2012) 990–992.

[41] E. L. Popova, V. I. Rozenberg, Z. A. Starikova, S. Keuker–Baumann, H. S. Kitzerow, H. Hopf, Thermotropic liquid crystals from planar chiral compounds: Optically active mesogenic [2.2]paracyclophane derivatives, *Angew. Chem. Int. Ed.* **41** (2002) 3411–3414.